Opposite-sign WW production with Run3 data in ATLAS

ALBERTO PLEBANI

IOP Joint APP and HEPP Annual Conference 2026

Edinburgh – 8th April 2026

Supervisor: Dr. Sarah Louise Williams

University of Cambridge, St Edmund's College

HARDING
Distinguished Postgraduate
SCHOLARS PROGRAMME

ATLAS
EXPERIMENT

Standard Model Physics at the LHC

- Standard Model tested across 7 orders of magnitude with good agreement with predictions

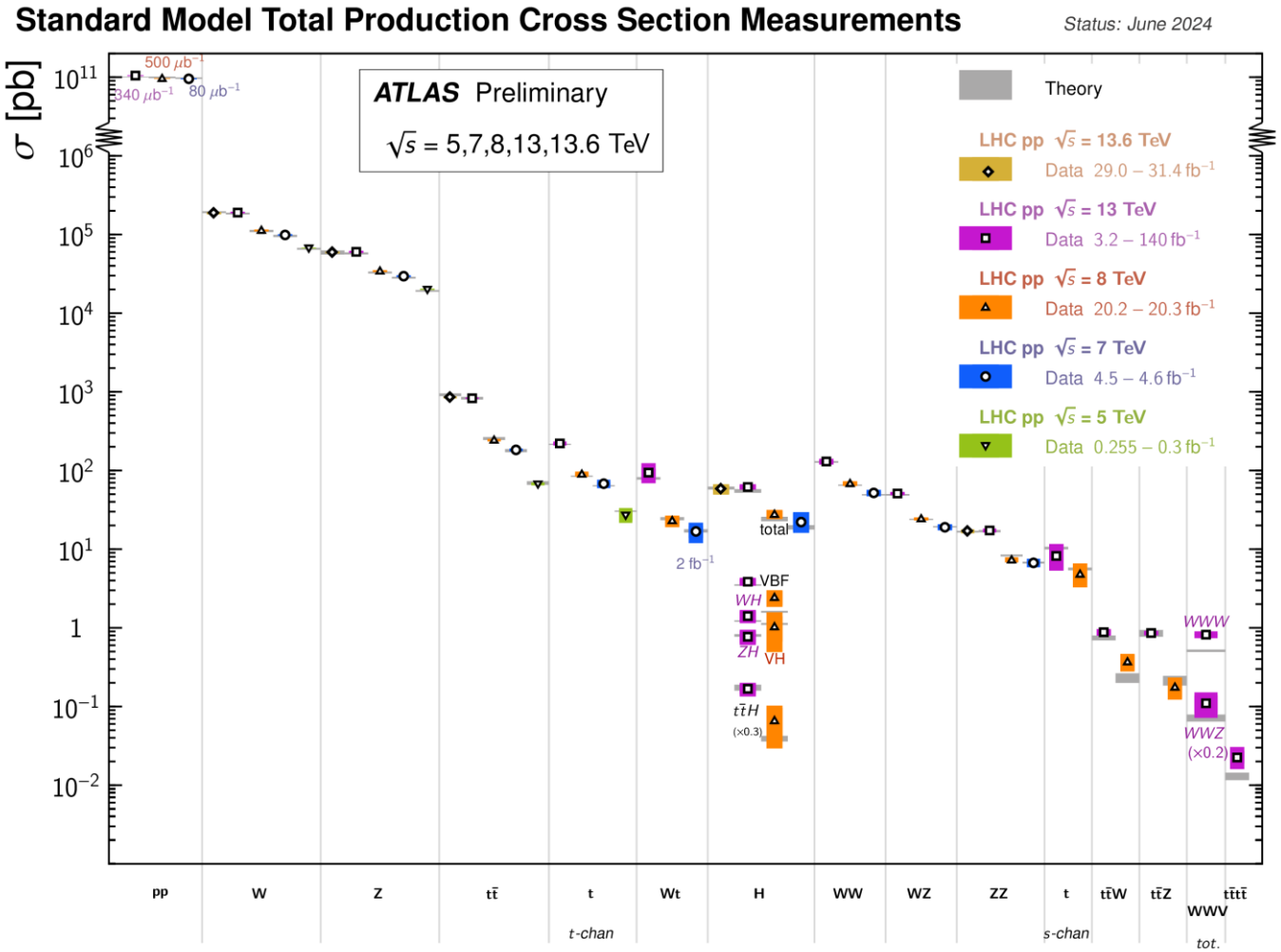

ATL-PHYS-PUB-2024-011

Standard Model Physics at the LHC

- Standard Model tested across 7 orders of magnitude with good agreement with predictions
- WW process:
  - Evidence in Run1 at $\sqrt{s} = 8$ TeV
  - Measurement in 2015 at $\sqrt{s} = 8$ TeV
  - Differential measurement at $\sqrt{s} = 13$ TeV with partial Run2 (36.1 fb^{-1})
  - Differential, EFT and asymmetry at $\sqrt{s} = 13$ TeV for full Run2 (140 fb^{-1})

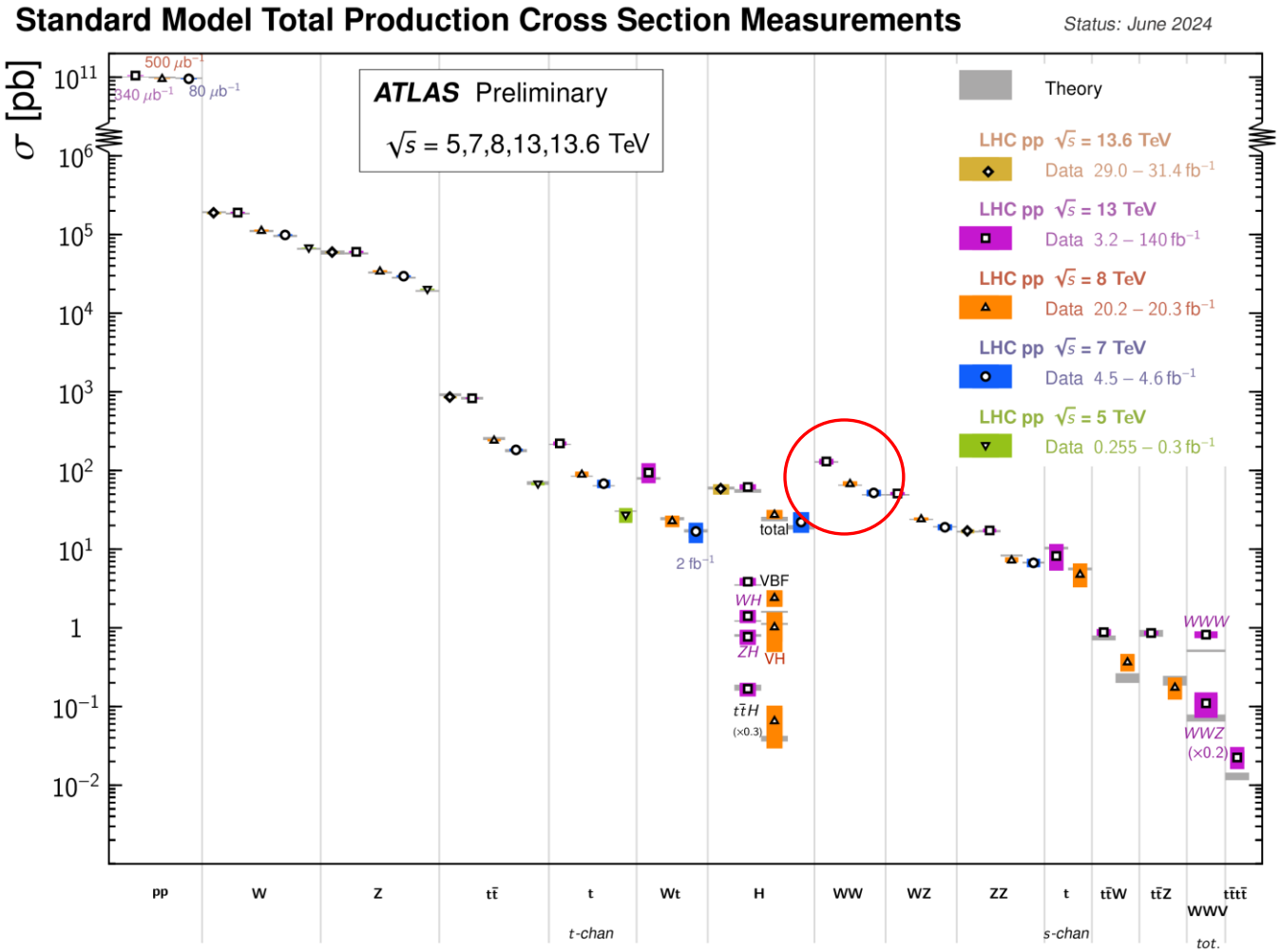

ATL-PHYS-PUB-2024-011

Standard Model Physics at the LHC

- Standard Model tested across 7 orders of magnitude with good agreement with predictions
- WW process:
  - Evidence in Run1 at $\sqrt{s} = 8$ TeV
  - Measurement in 2015 at $\sqrt{s} = 8$ TeV
  - Differential measurement at $\sqrt{s} = 13$ TeV with partial Run2 (36.1 fb^{-1})
  - Differential, EFT and asymmetry at $\sqrt{s} = 13$ TeV for full Run2 (140 fb^{-1})
- This analysis (team from Cambridge and Manchester)
  - First partial Run3 WW measurement at $\sqrt{s} = 13.6$ TeV (163.9 fb^{-1})
  - Differential measurement with focus on CP-Violation (CPV) and WW polarisation observables
  - Will also perform EFT interpretation

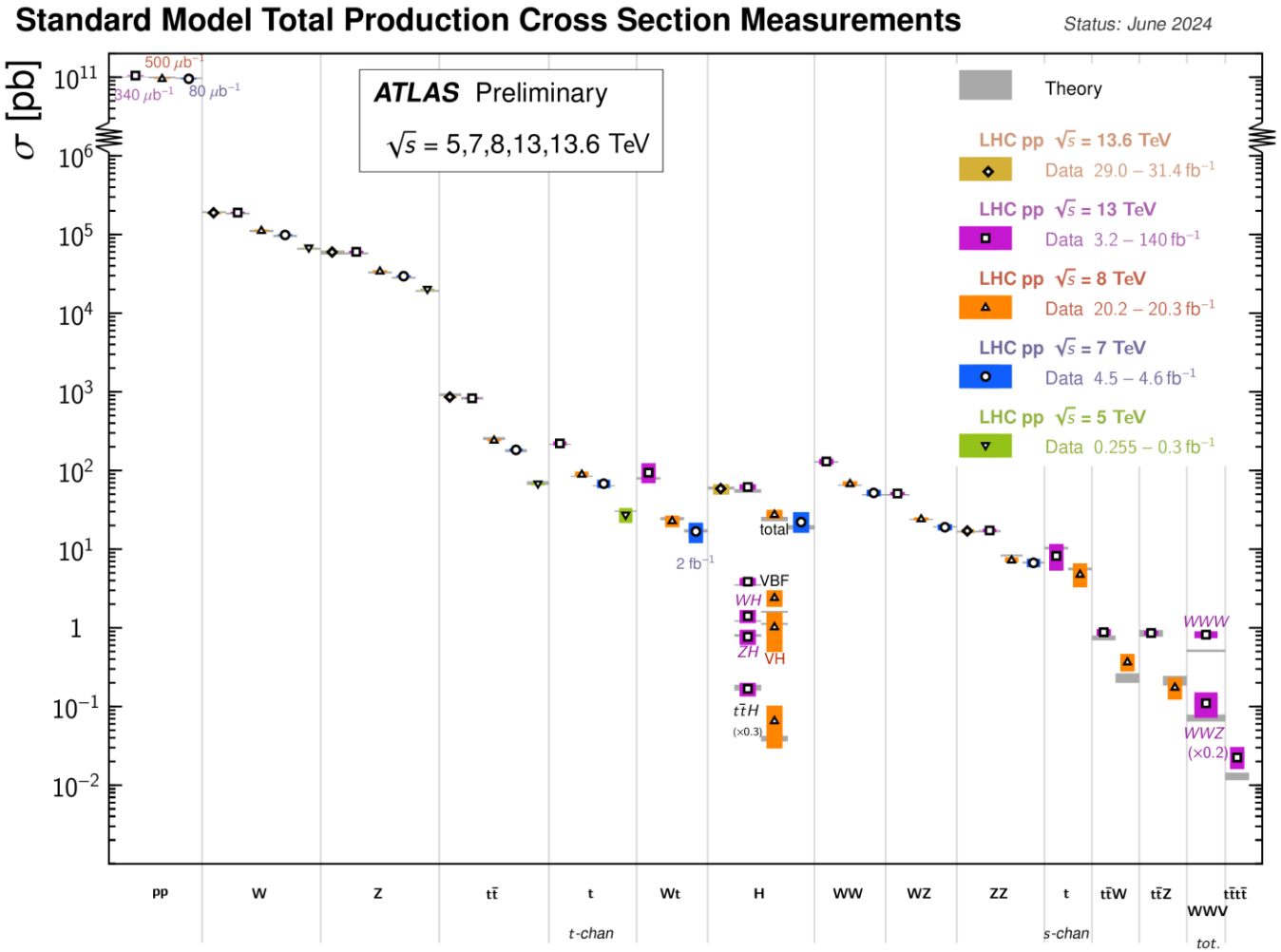

ATL-PHYS-PUB-2024-011

WW production

- Opposite-sign opposite-flavour WW final state

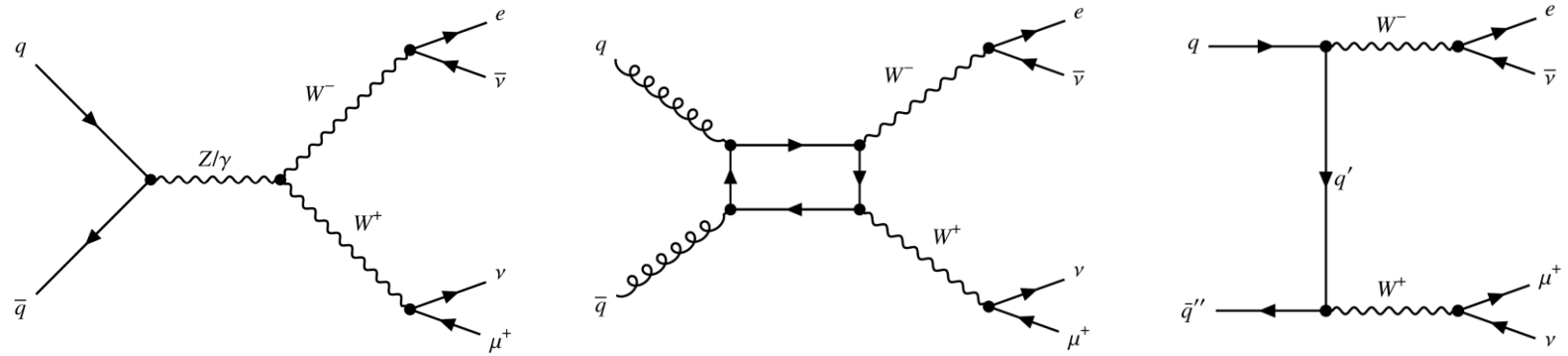

- Predicted cross section (Matrix 2.1 NNLO x NLO EW): $\sigma(W^+W^-) = 123 \pm 1$ (PDF) ± 2 (scale) fb

WW production

- Opposite-sign opposite-flavour WW final state

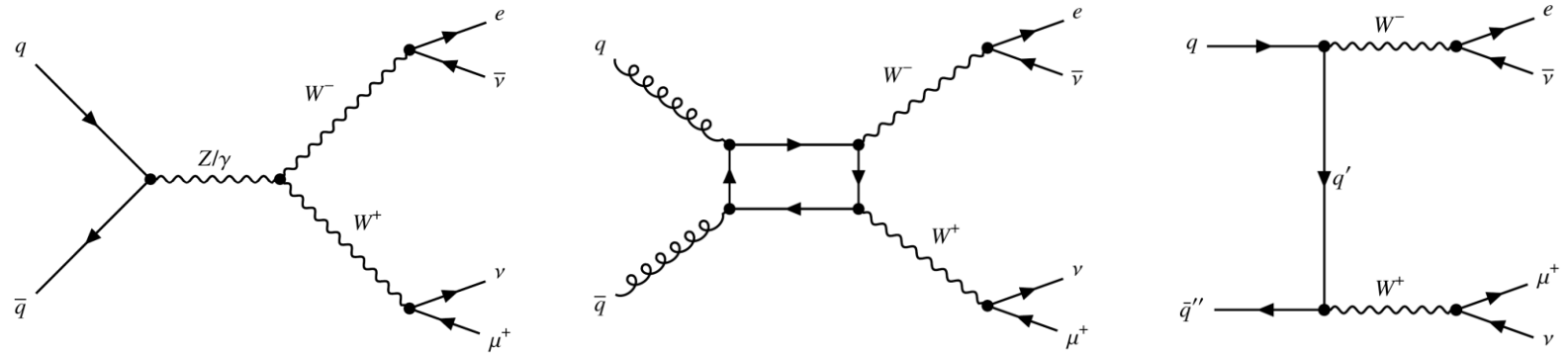

- Predicted cross section (Matrix 2.1 NNLO x NLO EW): $\sigma(W^+W^-) = 123 \pm 1$ (PDF) ± 2 (scale) fb

- Full Run2 analysis ($\sqrt{s}$ =13 TeV, 140 fb^{-1}):
  - Inclusive cross-section $\sigma\left(W^+W^- \to e^{\pm}\nu\,\mu^{\mp}\nu\right) = 127 \pm 1\,(stat.) \pm 4\,(syst.)$ fb
  - Differential cross section measured as a function of kinematic variables

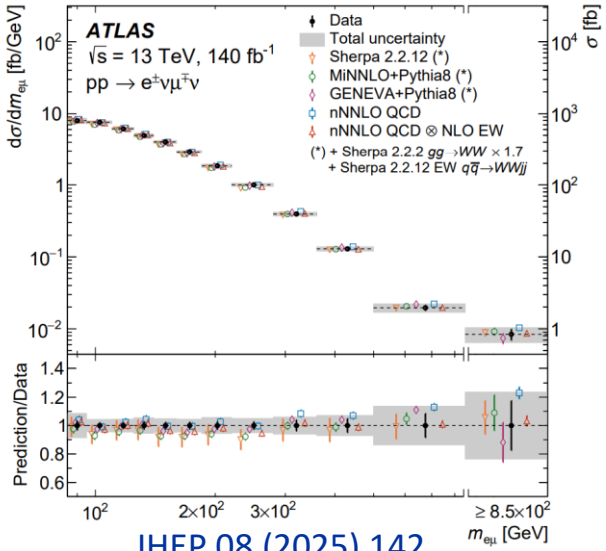

JHEP 08 (2025) 142

WW production

- Opposite-sign opposite-flavour WW final state

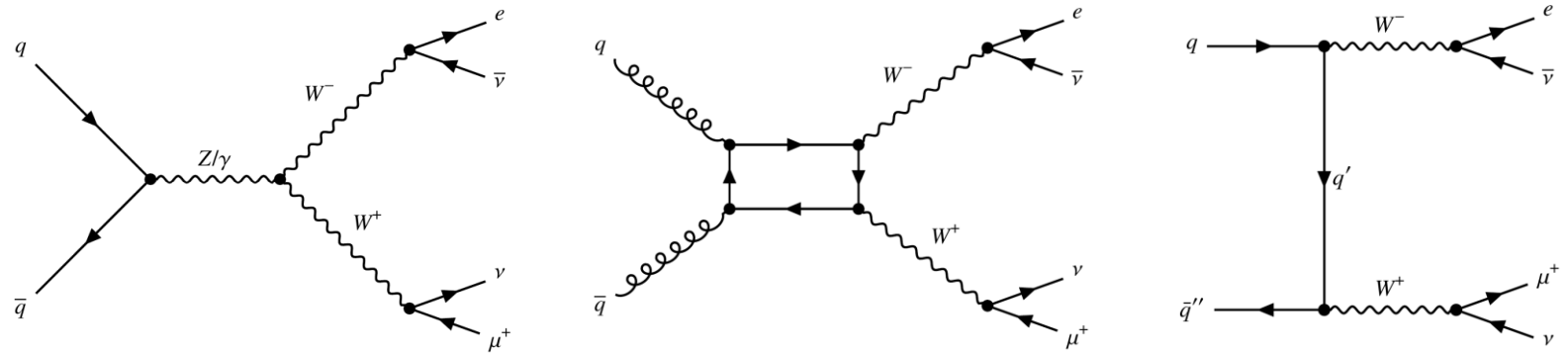

- Predicted cross section (Matrix 2.1 NNLO x NLO EW): $\sigma(W^+W^-) = 123 \pm 1$ (PDF) ± 2 (scale) fb

- Full Run2 analysis ($\sqrt{s}$ =13 TeV, 140 fb^{-1}):
  - Inclusive cross-section $\sigma\left(W^+W^- \to e^{\pm}\nu\,\mu^{\mp}\nu\right) = 127 \pm 1\,(stat.) \pm 4\,(syst.)$ fb
  - Differential cross section measured as a function of kinematic variables

- Partial Run3 analysis ($\sqrt{s}$ =13.6 TeV, 163.9 fb^{-1} :
  - Goal is to unfold variables sensitive to CPV and= WW polarisation
  - First look at CP-odd observables (signed $\Delta\phi(\ell\ell)$)
  - Enhance sensitivity to linear EFT over previous measurements
    - In particular Triple Gauge Coupling

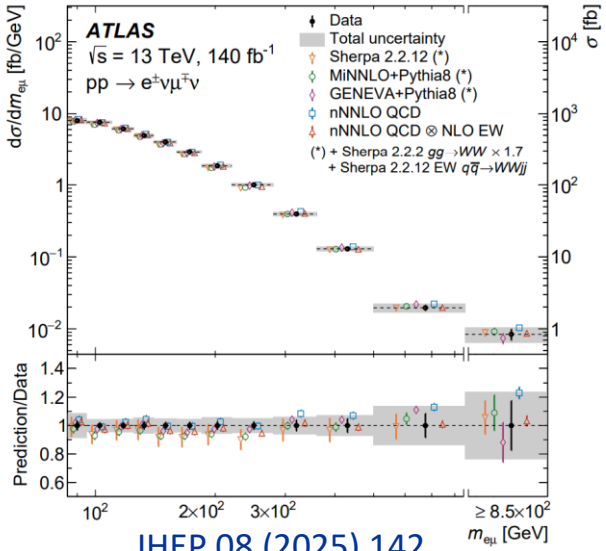

JHEP 08 (2025) 142

Event selection

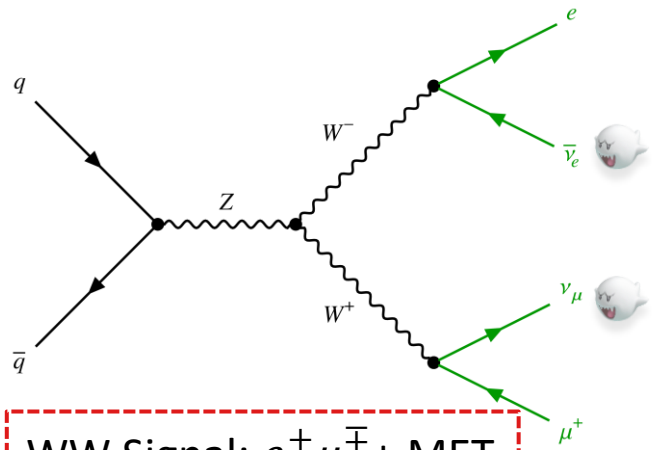

WW Signal: $e^{\pm}\mu^{\mp}$+ MET

Event selection

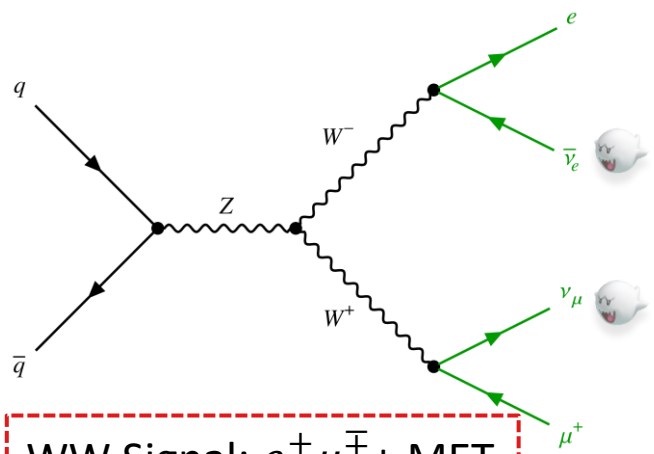

WW Signal: $e^{\pm}\mu^{\mp}$+ MET

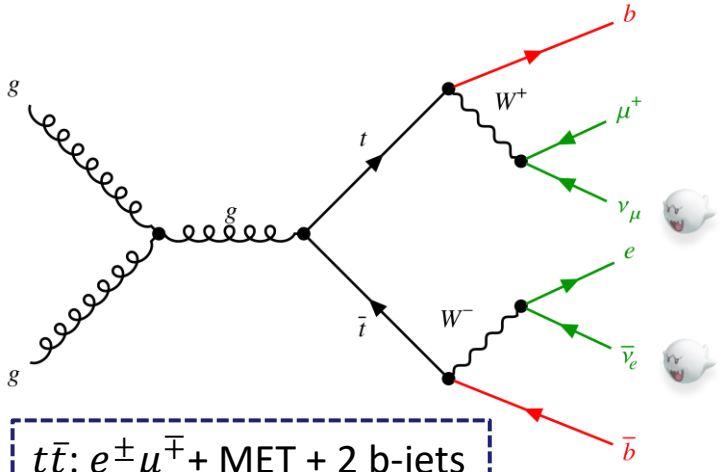

$t\bar{t}$: $e^{\pm}\mu^{\mp}$+ MET + 2 b-jets
=> b-jet veto

Event selection

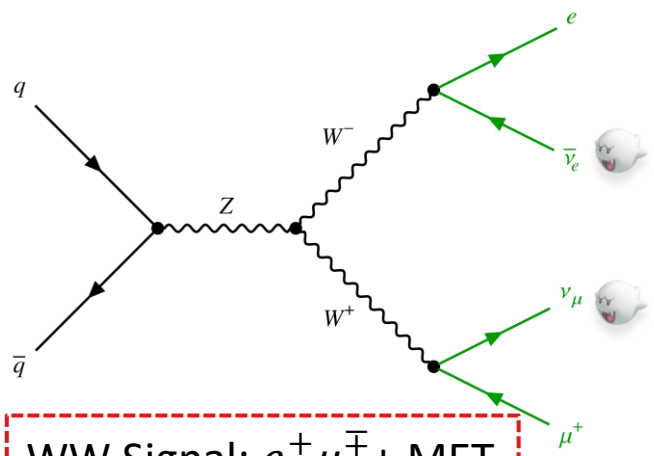

WW Signal: $e^{\pm}\mu^{\mp}$+ MET

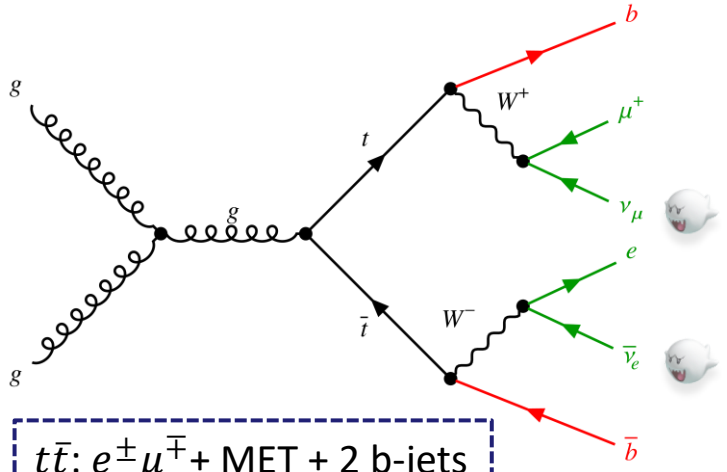

$t\bar{t}$: $e^{\pm}\mu^{\mp}$+ MET + 2 b-jets
=> b-jet veto

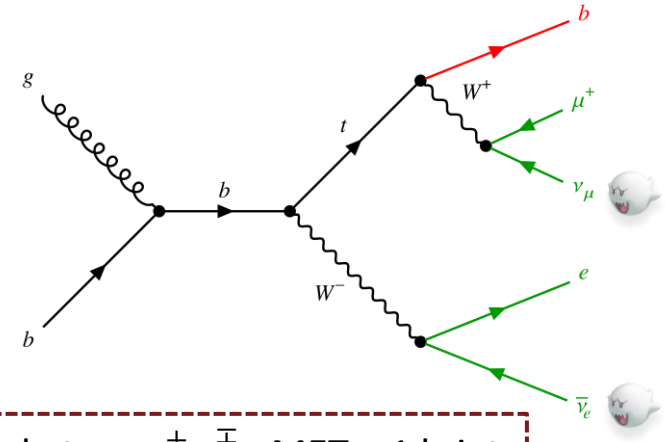

Single top: $e^{\pm}\mu^{\mp}$+ MET + 1 b-jet
=> b-jet veto

Event selection

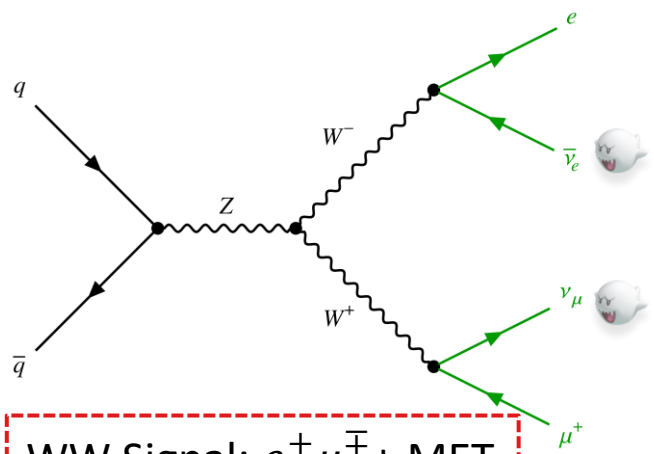

WW Signal: $e^{\pm}\mu^{\mp}$+ MET

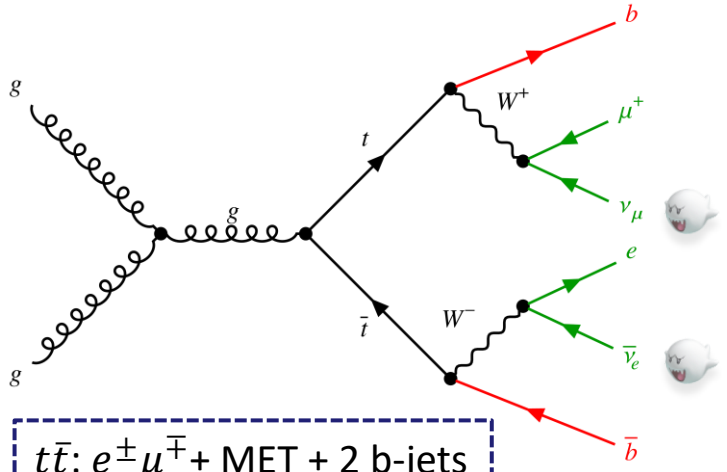

$t\bar{t}$: $e^{\pm}\mu^{\mp}$+ MET + 2 b-jets
=> b-jet veto

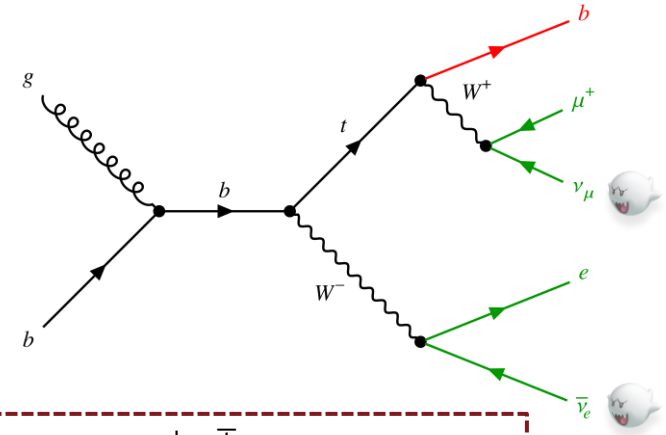

Single top: $e^{\pm}\mu^{\mp}$+ MET + 1 b-jet
=> b-jet veto

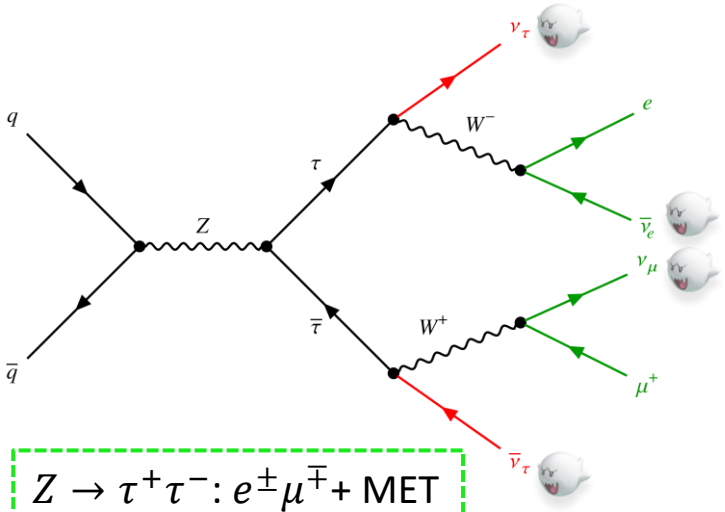

$Z \to \tau^{+}\tau^{-}$: $e^{\pm}\mu^{\mp}$+ MET
-> mll > 100 GeV

Event selection

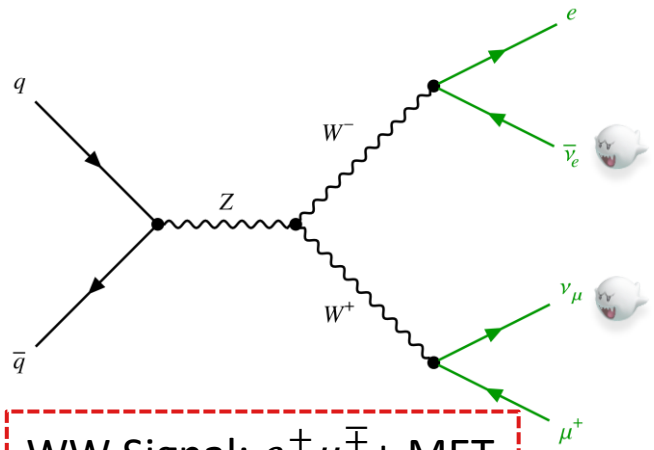

WW Signal: $e^{\pm}\mu^{\mp}$+ MET

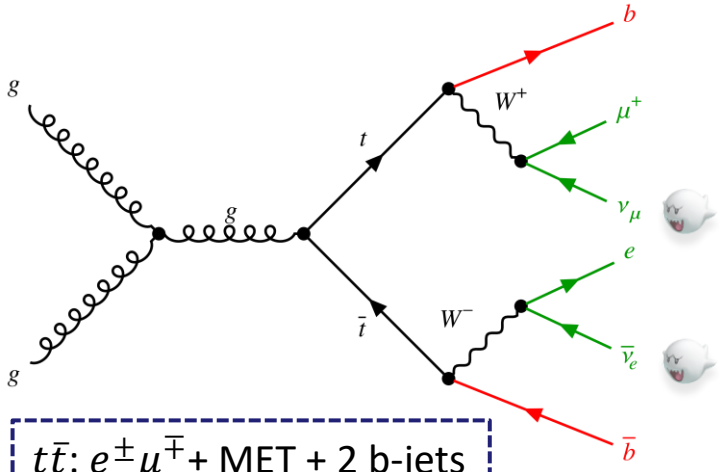

$t\bar{t}$: $e^{\pm}\mu^{\mp}$+ MET + 2 b-jets
=> b-jet veto

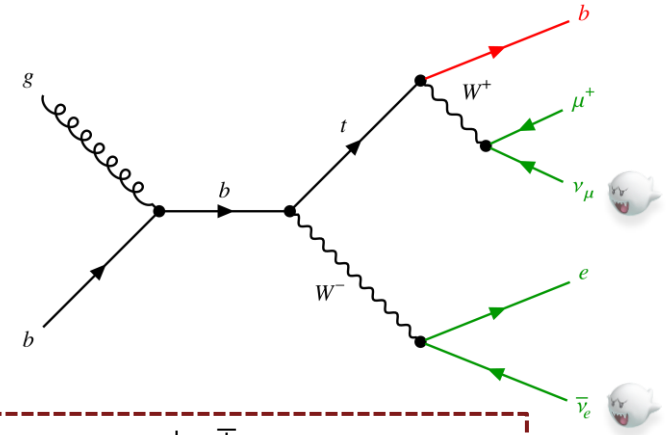

Single top: $e^{\pm}\mu^{\mp}$+ MET + 1 b-jet
=> b-jet veto

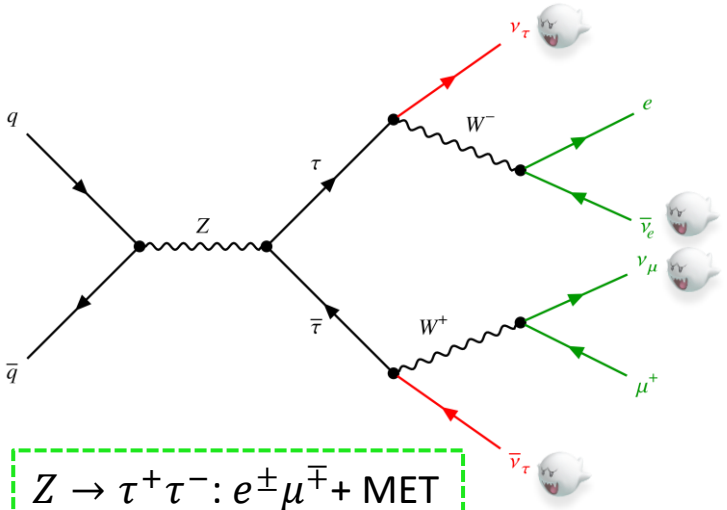

$Z \to \tau^{+}\tau^{-}$: $e^{\pm}\mu^{\mp}$+ MET
-> mll > 100 GeV

Sample	Yields ± Stat.	Percentage (%)
WW	57 485.7 ± 77.2	34.0
$Z + jets$	3636.5 ± 324.4	2.2
WZ	2366.5 ± 9.2	1.4
VV	130.6 ± 1.1	0.1
$t\bar{t}$	77 451.1 ± 762.8	45.8
$V\gamma$	174.1 ± 25.5	0.1
$W + jets$	100.7 ± 64.6	0.1
VVV	201.1 ± 0.5	0.1
VV EWK	768.0 ± 9.0	0.5
Single-top	19 748.4 ± 28.8	11.7
Fakes	6877.6 ± 72.4	4.1
Total mc23ade	168 940.4 ± 839.2	1
Run 3 Data	170 773.0 ± 413.2	-
Data/MC	1.01	-

Good data/MC agreement

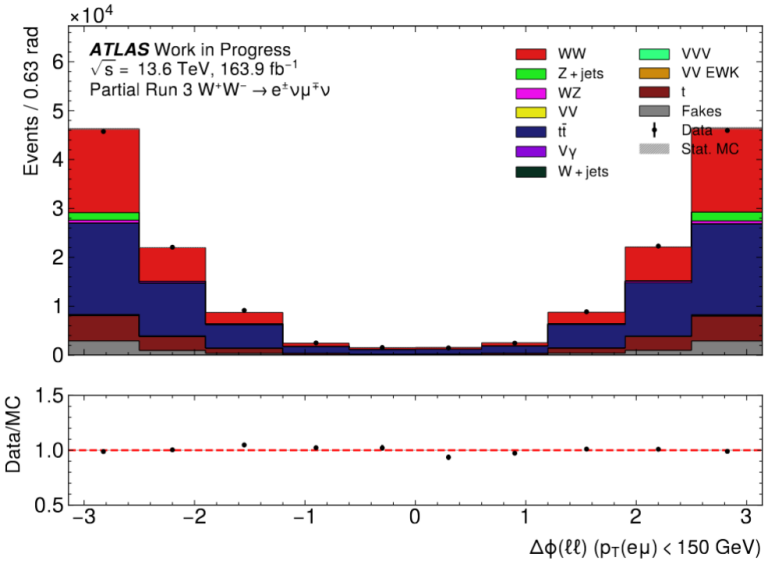

ATLAS detector effects

- ATLAS has a finite detector acceptance and resolution
- These effects lead to mismeasurements of the final state objects, which make it harder to compare with the truth-level prediction

Crack veto region: no electrons

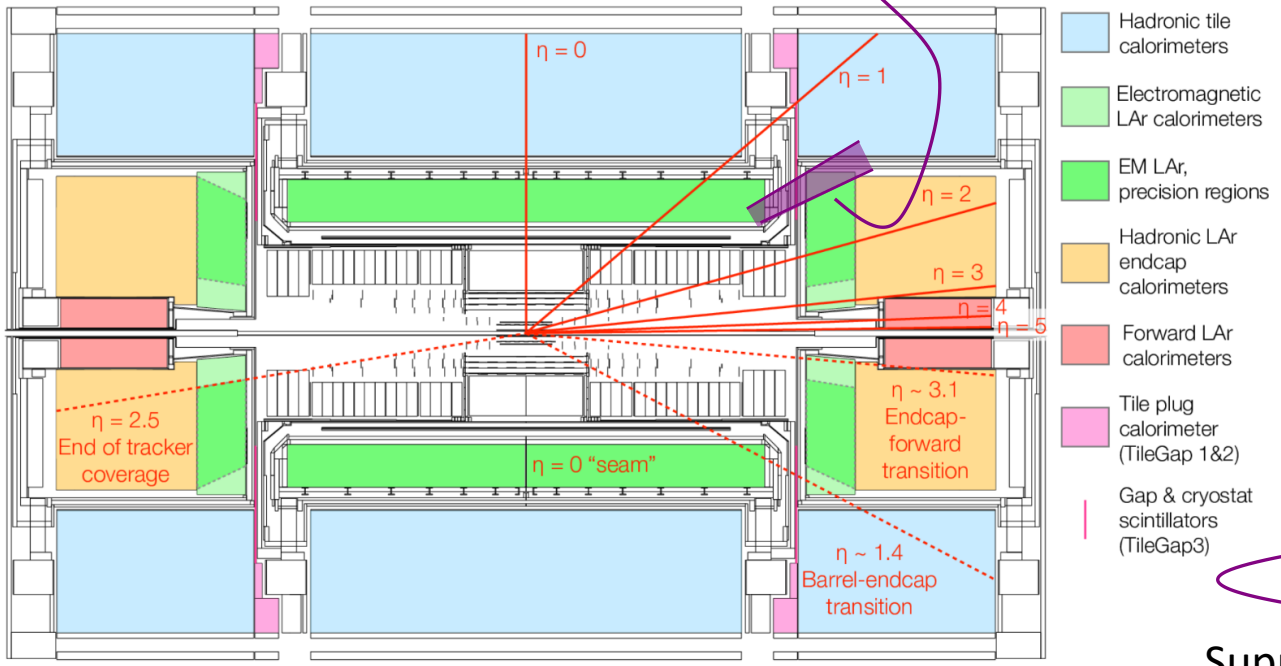

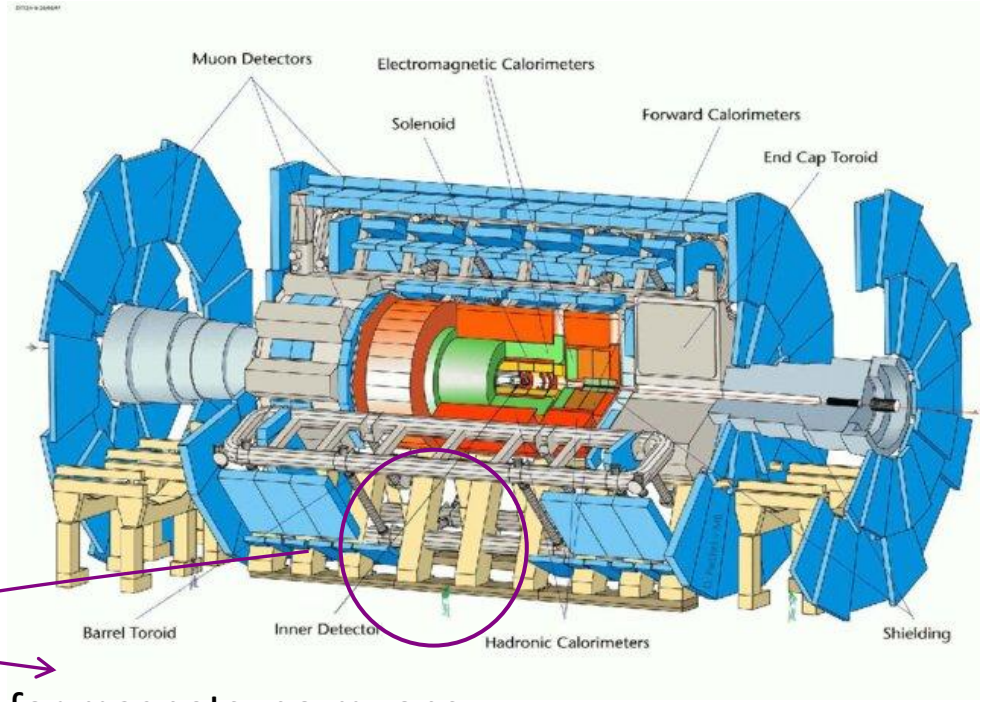

Support for magnets: no muons

Unfolding

- Unfolding: correcting the measured distribution to account for the detector's effects

Unfolding

- Unfolding: correcting the measured distribution to account for the detector's effects
- The unfolding procedure can be parametrised as follows:
  - Response matrix: probability of measuring an event in reco given the event is measured in truth
  - Migration matrix: probability of observing both reco and truth
  - Reconstruction efficiency: probability of measuring reco
  - Fiducial acceptance : probability of measuring truth

$$\varepsilon = \frac{N(T \cap R,\ \text{reco}\ \omega)}{N(T,\ \text{truth}\ \omega)}$$

$$\alpha = \frac{N(T \cap R,\ \text{reco}\ \omega)}{N(R,\ \text{reco}\ \omega)}$$

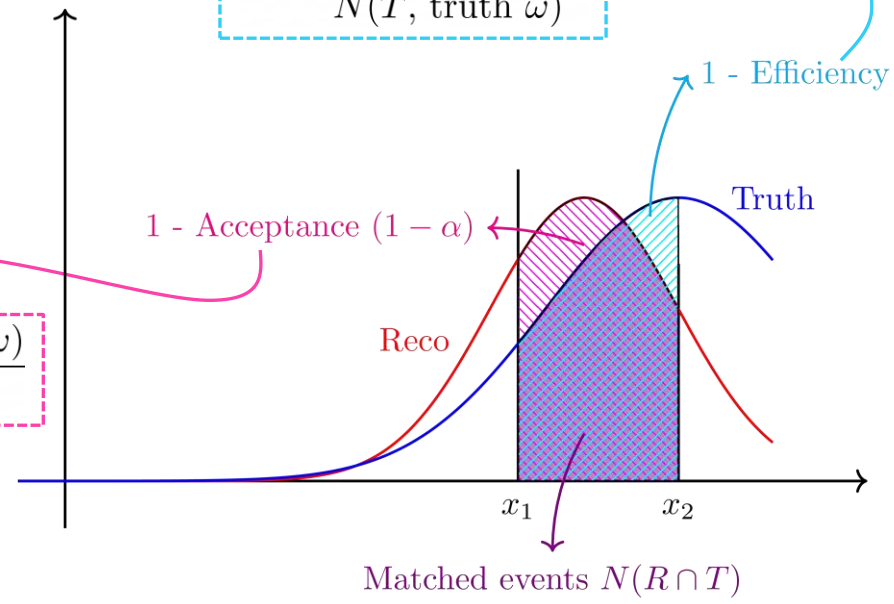

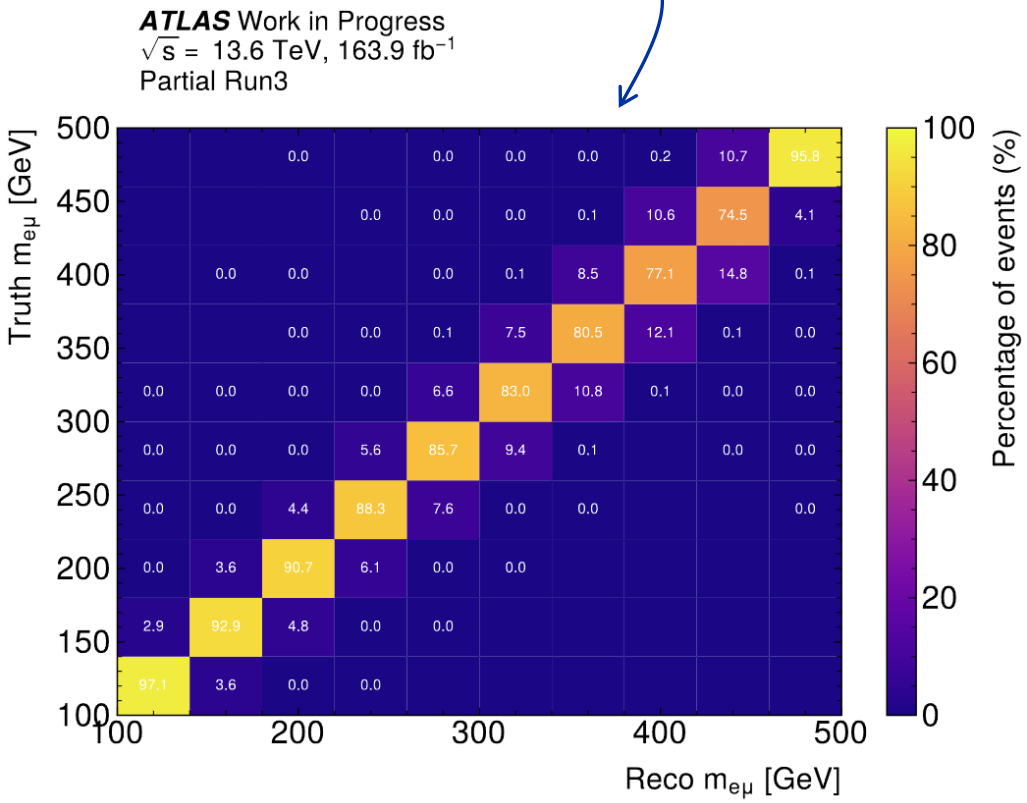

Reco-level data analysis workflow

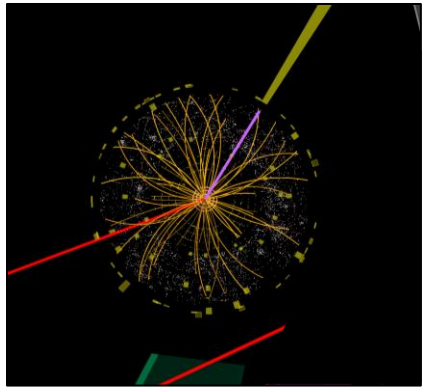

Collision

Reco-level data analysis workflow

Detector interaction

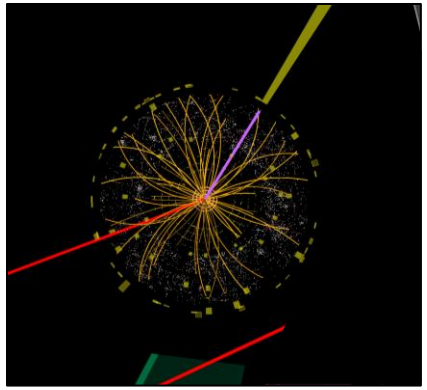

Collision

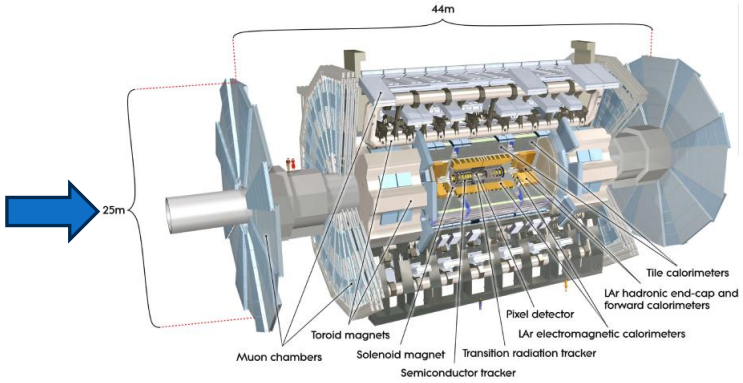

Reco-level data analysis workflow

Detector interaction

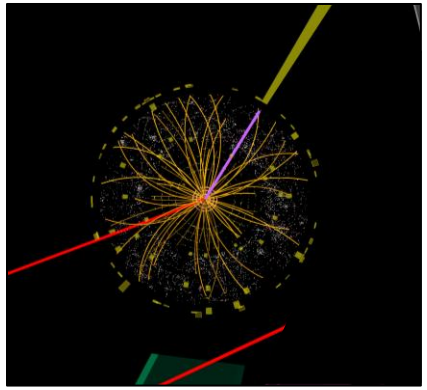

Collision

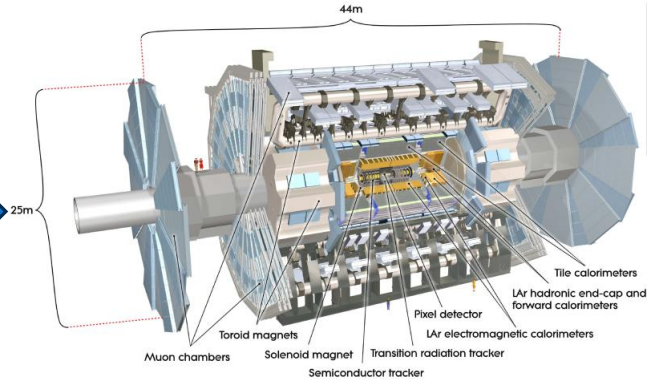

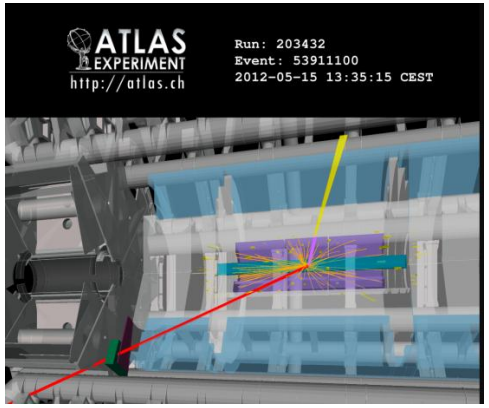

Detector reconstruction

Reco-level data analysis workflow

Detector interaction

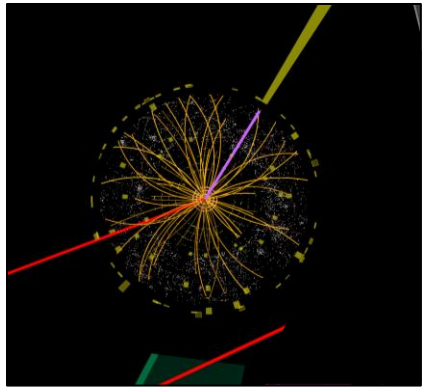

Collision

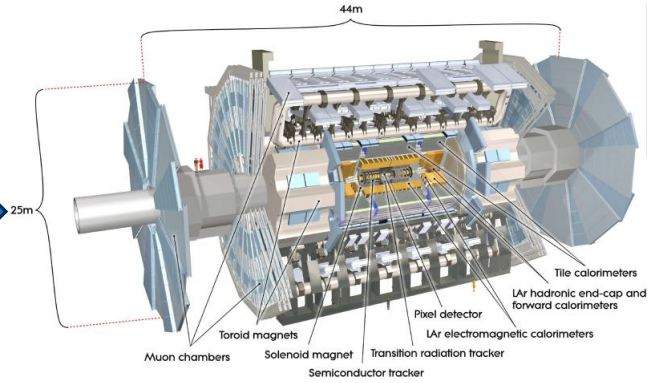

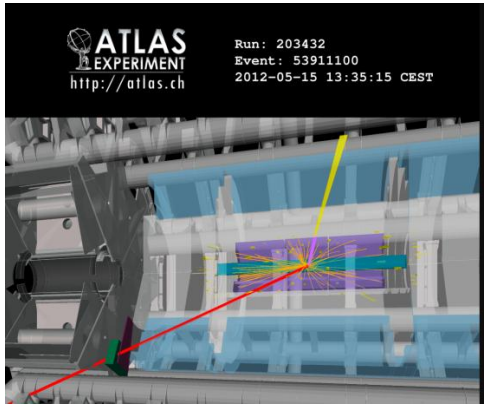

Detector reconstruction

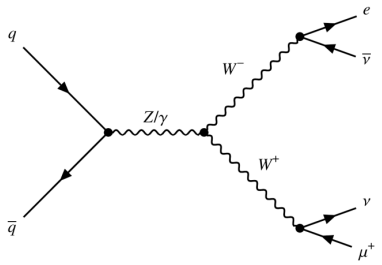

Physics model

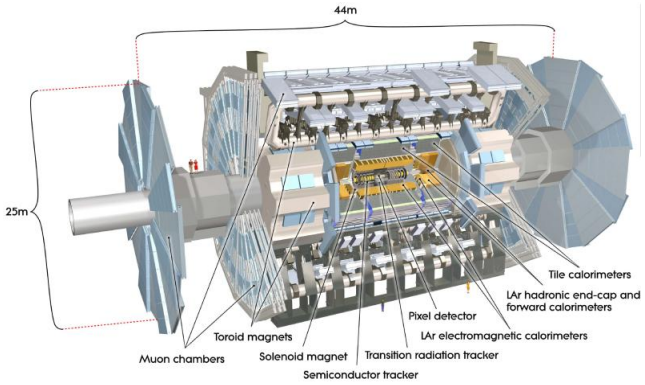

Detector simulation

Reco-level data analysis workflow

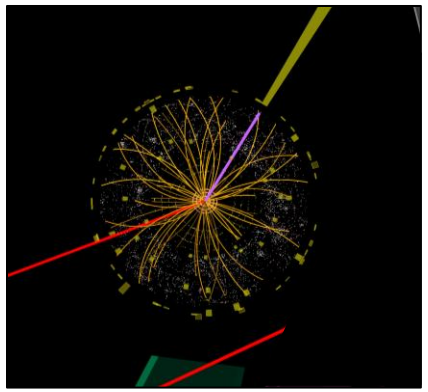

Collision

Detector interaction

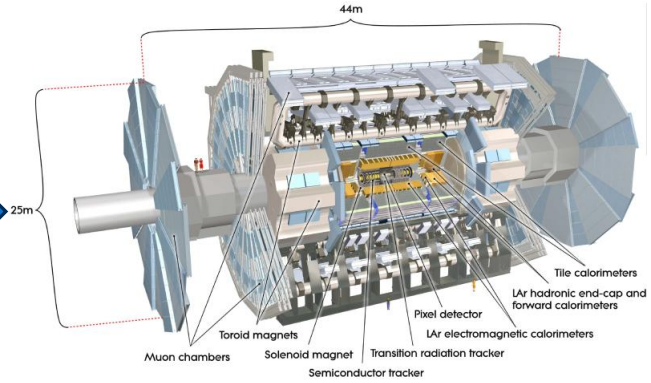

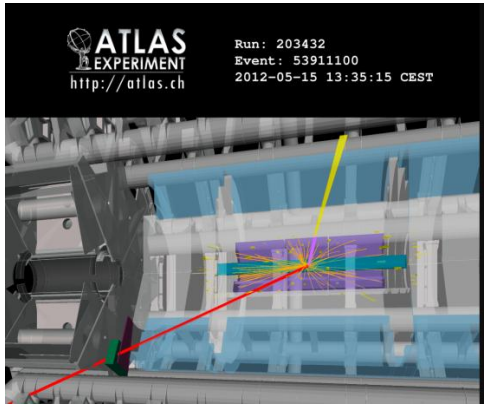

Detector reconstruction

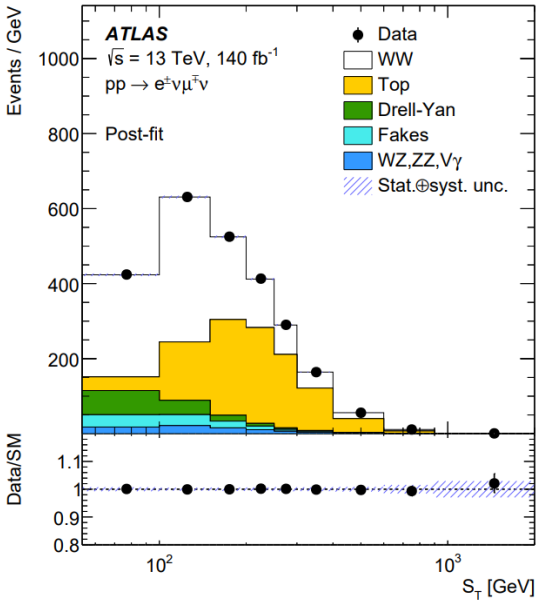

Analysis

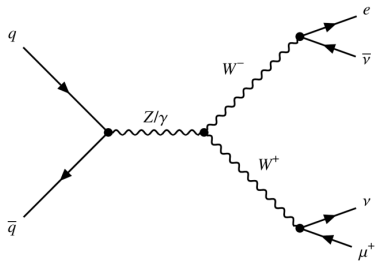

Physics model

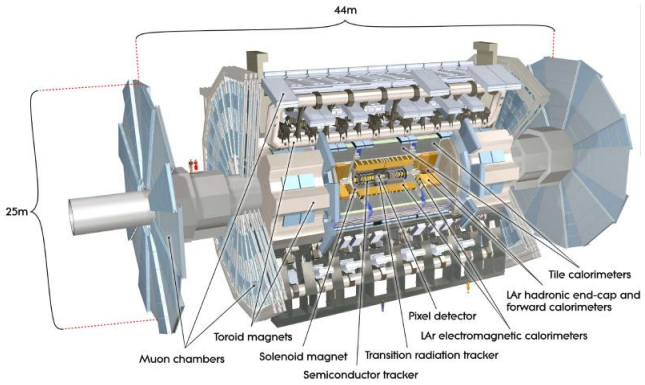

Detector simulation

Unfolding analysis workflow

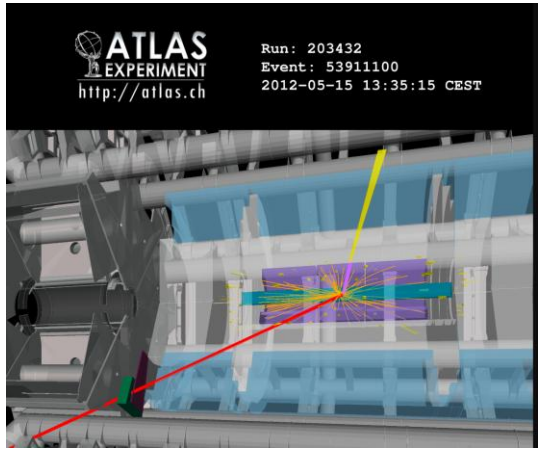

Detector reconstruction

Unfolding analysis workflow

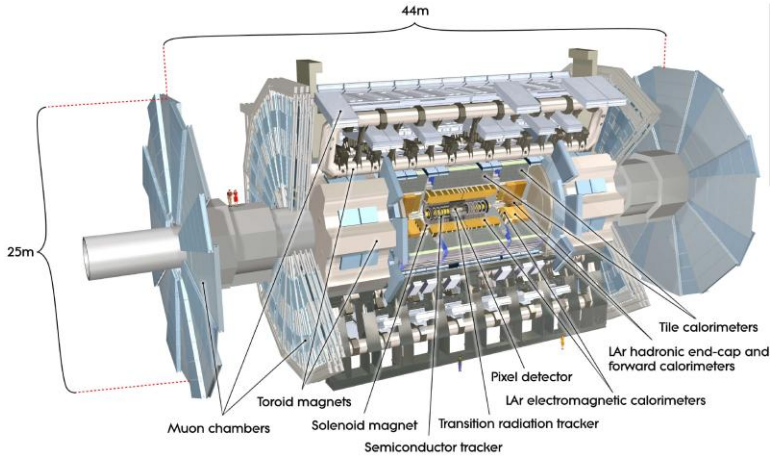

Detector simulation

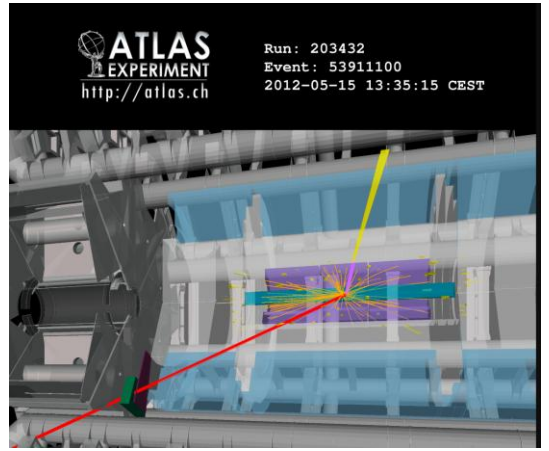

Detector reconstruction

Unfolding analysis workflow

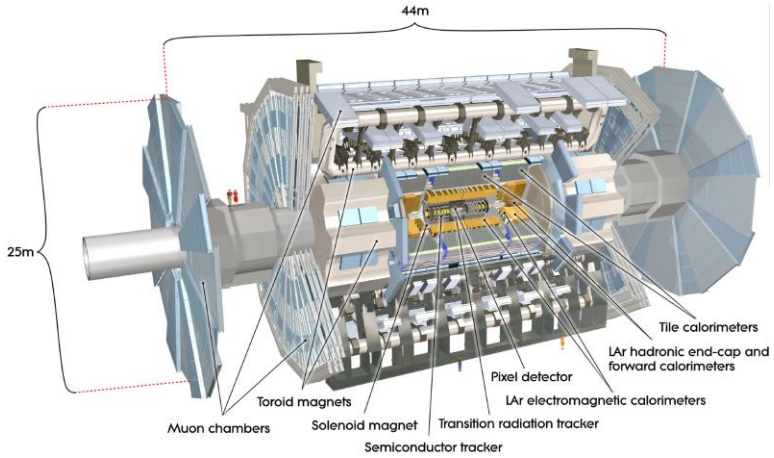

Detector simulation

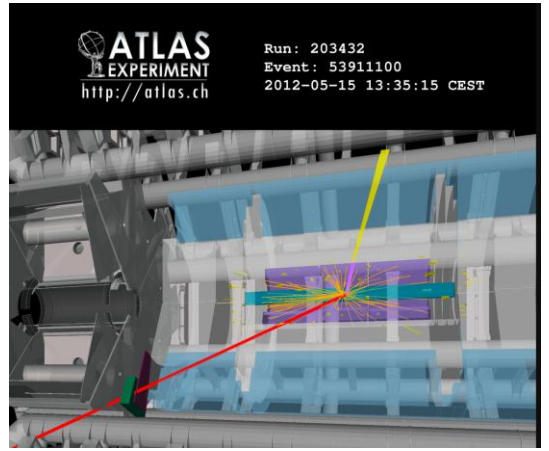

Detector reconstruction

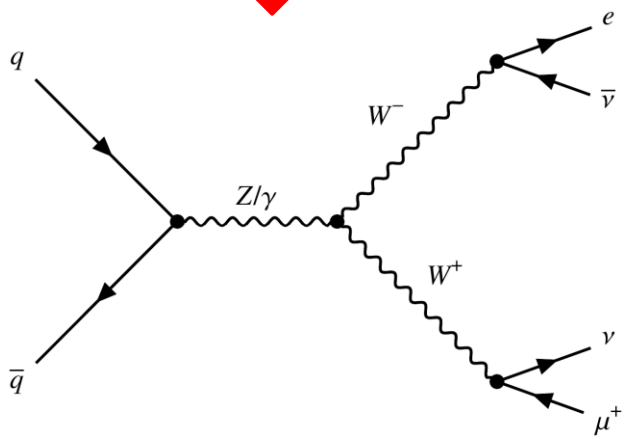

Physics model

Unfolding analysis workflow

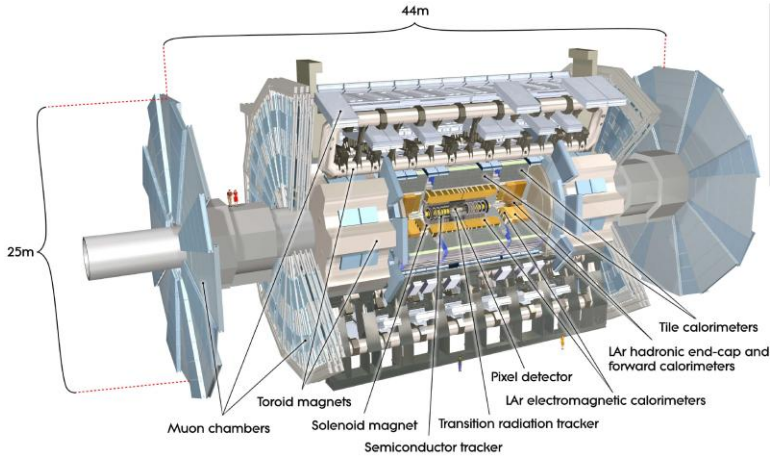

Detector simulation

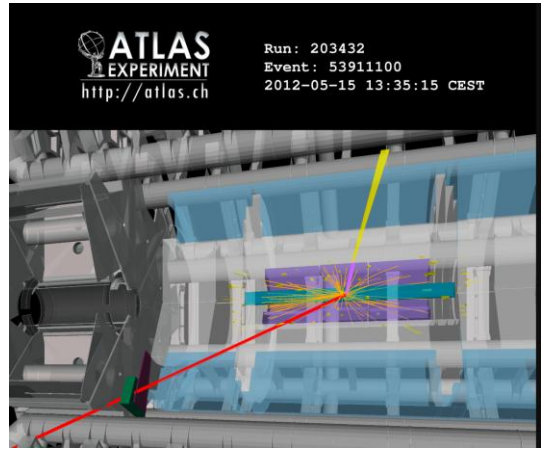

Detector reconstruction

Unfolding

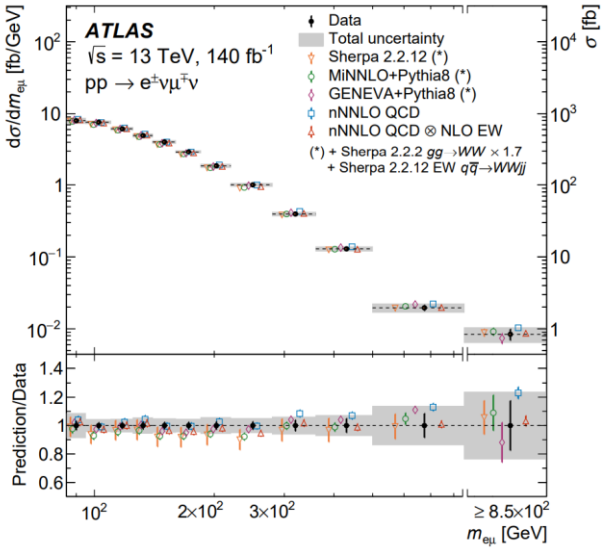

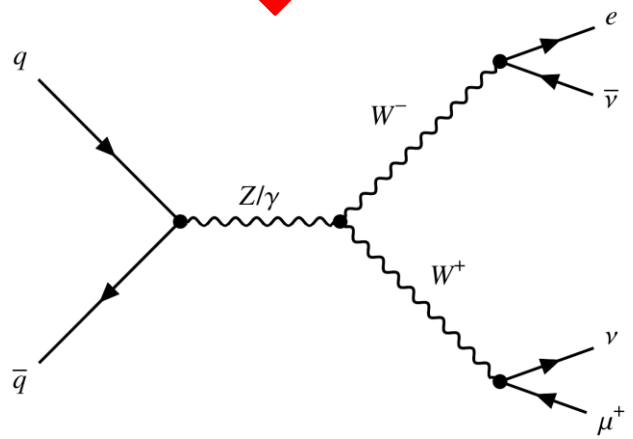

Physics model

Variables to unfold

- Unfolding variables which are sensitive to polarisation and potential BSM effects, particularly EFT

Variable	Description	Motivation
$p_T(\ell_1)$	p_T of the leading lepton	Interesting for single-boson polarisation studies
E_T^{miss}	Missing transverse energy	Unfolded in previous WW analyses
$m_{e\mu}$	Invariant mass of the electron-muon pair	Provides sensitivity to EFT and polarisation of the WW system
$p_T(e,\mu)$	Transverse momentum of the electron-muon pair	Provides sensitivity to PDFs, EFT and polarisation of the WW system
$\Delta\eta(\ell\ell)$	Pseudorapidity difference between rapidity-ordered leptons	Sensitive to CP-odd operators
$\Delta\phi(\ell\ell)$	Azimuthal difference between rapidity-ordered leptons	Sensitive to CP-odd operators, showed a mild tension with SM
$p_T(e,\mu)$ vs $\Delta\phi(\ell\ell)$	Double-differential cross section	Study $\Delta\phi(\ell\ell)$ only in the high-p_T region, where EFT effects rise

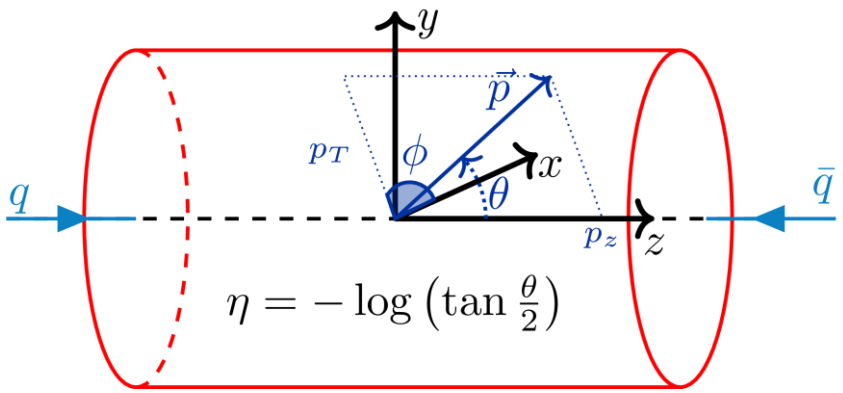

ATLAS coordinate system

Variables to unfold

- Unfolding variables which are sensitive to polarisation and potential BSM effects, particularly EFT

Variable	Description	Motivation
$p_T(\ell_1)$	p_T of the leading lepton	Interesting for single-boson polarisation studies
E_T^{miss}	Missing transverse energy	Unfolded in previous WW analyses
$m_{e\mu}$	Invariant mass of the electron-muon pair	Provides sensitivity to EFT and polarisation of the WW system
$p_T(e,\mu)$	Transverse momentum of the electron-muon pair	Provides sensitivity to PDFs, EFT and polarisation of the WW system
$\Delta\eta(\ell\ell)$	Pseudorapidity difference between rapidity-ordered leptons	Sensitive to CP-odd operators
$\Delta\phi(\ell\ell)$	Azimuthal difference between rapidity-ordered leptons	Sensitive to CP-odd operators, showed a mild tension with SM
$p_T(e,\mu)$ vs $\Delta\phi(\ell\ell)$	Double-differential cross section	Study $\Delta\phi(\ell\ell)$ only in the high-p_T region, where EFT effects rise

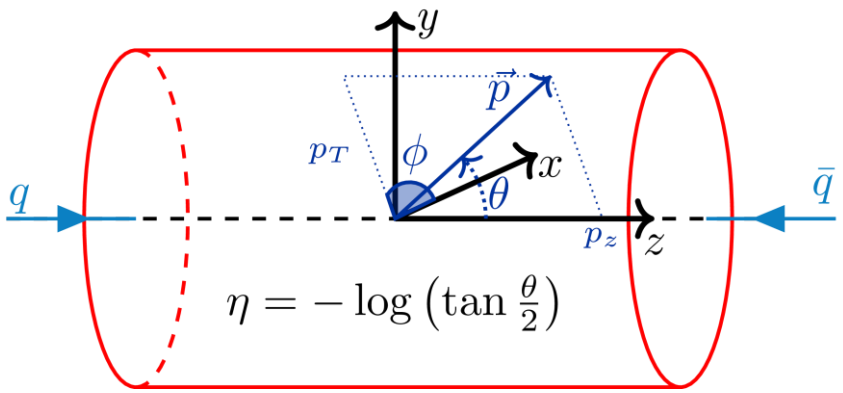

ATLAS coordinate system

$\Delta\phi(\ell\ell)$ for $O_{\widetilde{W}}$

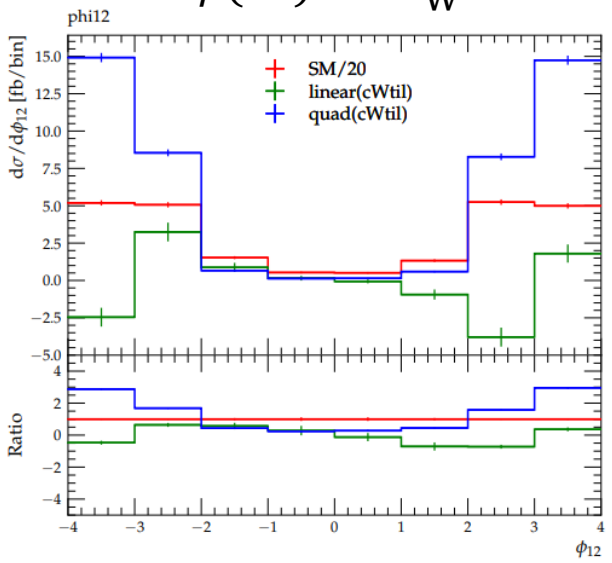

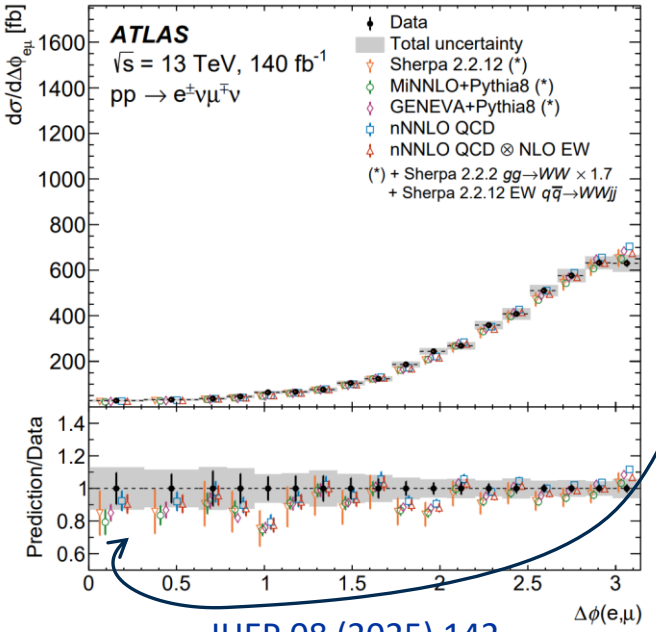

JHEP 08 (2025) 142

Unfolding $\Delta\phi(\ell\ell)$ vs $p_T(\ell\ell)$

- Low-$p_T(\ell\ell)$ bin: $0 \leq p_T(\ell\ell) \leq 150$ GeV

Unfolding $\Delta\phi(\ell\ell)$ vs $p_T(\ell\ell)$

- Low-$p_T(\ell\ell)$ bin: $0 \leq p_T(\ell\ell) \leq 150$ GeV
- Bin optimisation:
  - $\geq 70\%$ diagonal in Migration Matrix (limit migration) and ≥ 400 signal events per bin
  - Fiducial and Acceptance (left) and Migration Matrix (right)

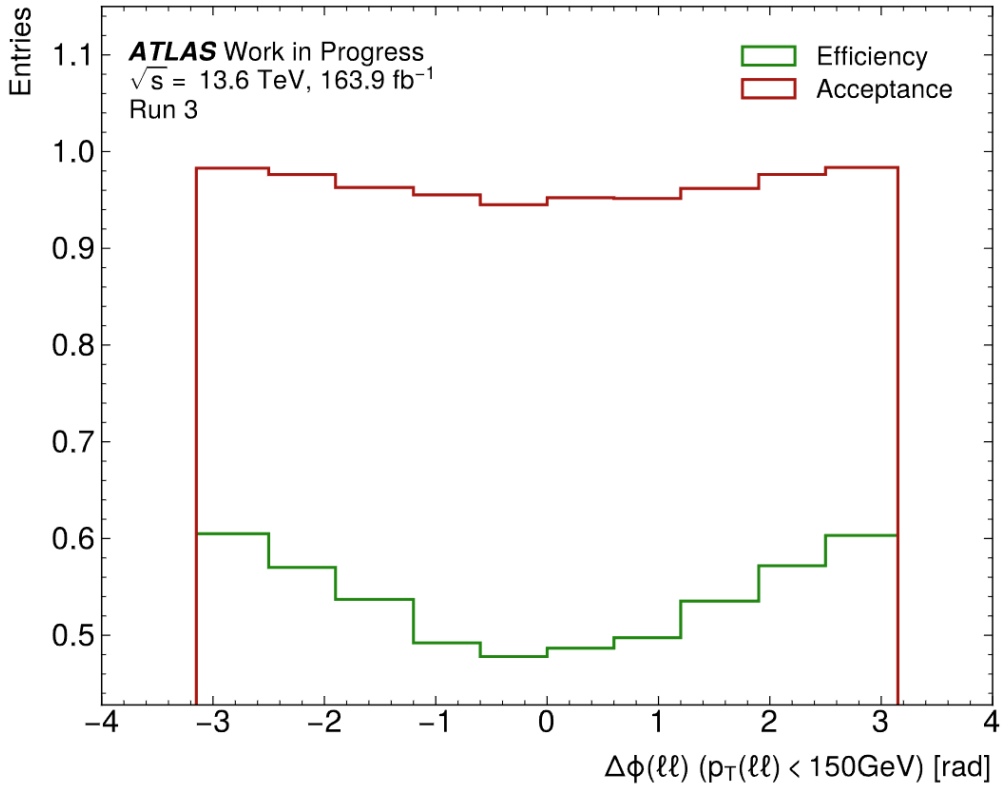

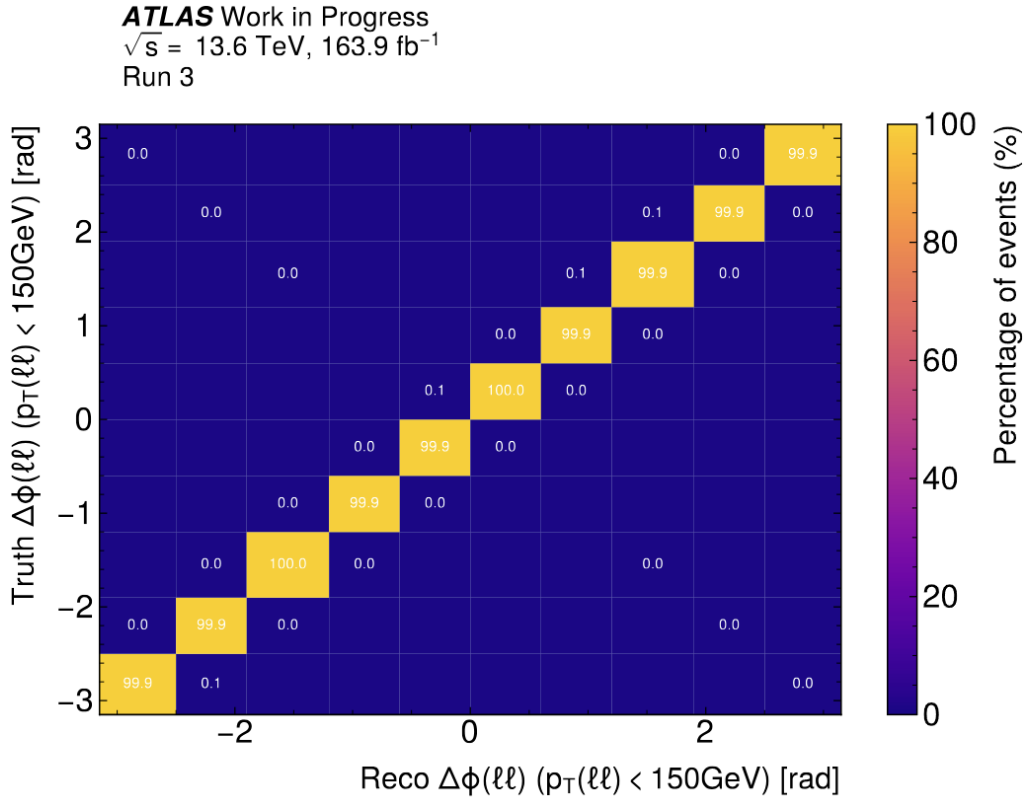

Signal truth: variations

- Renormalisation and factorisation scale:
  - μ_R affects α_S directly $\alpha_S(\mu_R^2) = \frac{\alpha_S(\mu_0^2)}{1 + \beta_0 \alpha_S(\mu_0)^2 \ln \frac{\mu_R^2}{\mu_0^2}}$
  - μ_F affects PDFs

Signal truth: variations

- Renormalisation and factorisation scale:
  - μ_R affects α_S directly $\alpha_S(\mu_R^2) = \dfrac{\alpha_S(\mu_0^2)}{1 + \beta_0 \alpha_S(\mu_0)^2 \ln \frac{\mu_R^2}{\mu_0^2}}$
  - μ_F affects PDFs
- Evaluated as 7-point envelope

$$\{(\mu_R,\ \mu_F)\} = \{(0.5, 0.5); (0.5, 1); (1, 0.5); (1, 1); (2, 1); (1, 2); (2, 2)\}$$

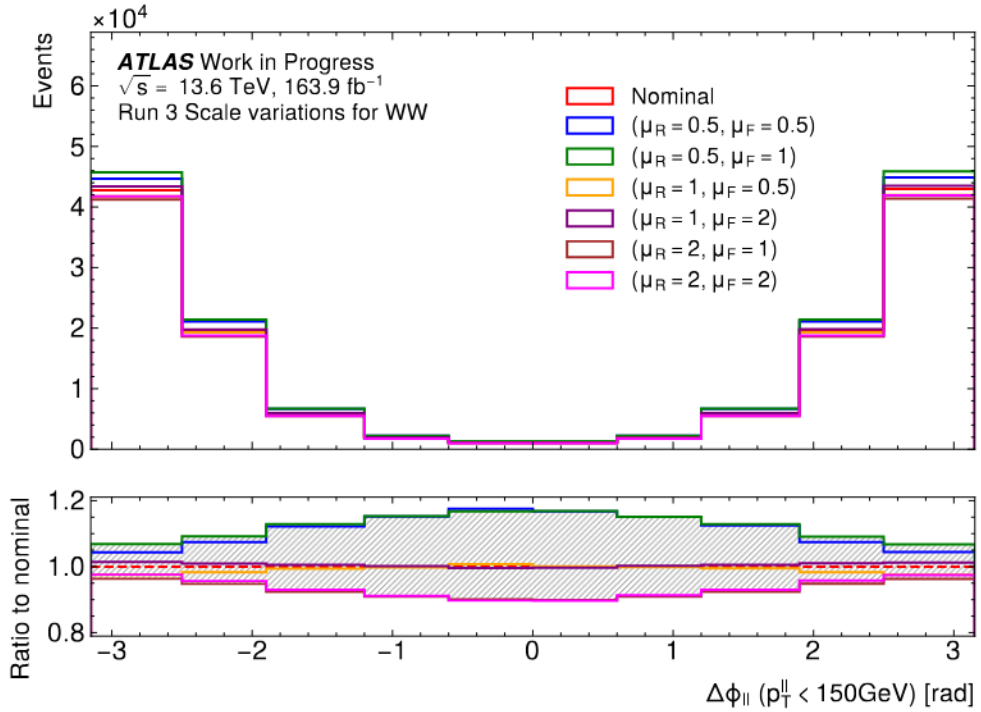

Signal truth: variations

- Renormalisation and factorisation scale:
  - μ_R affects α_S directly $\alpha_S(\mu_R^2) = \frac{\alpha_S(\mu_0^2)}{1 + \beta_0 \alpha_S(\mu_0)^2 \ln \frac{\mu_R^2}{\mu_0^2}}$
  - μ_F affects PDFs
- Evaluated as 7-point envelope

$$\{(\mu_R,\ \mu_F)\} = \{(0.5, 0.5); (0.5, 1); (1, 0.5); (1, 1); (2, 1); (1, 2); (2, 2)\}$$

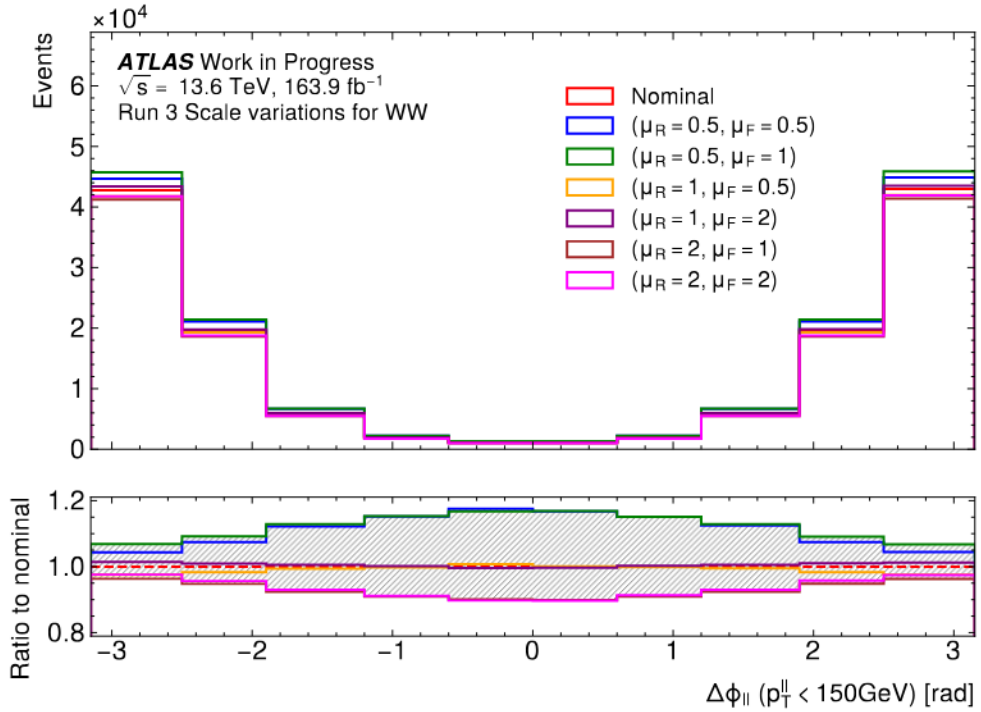

- PDF and α_S:
  - Using [PDF4LHC21 recommendations]
    - PDF uncertainty evaluated through 100 variations
    - α_S varied between 0.118 (nominal) $\pm$ 0.001
    - Two uncertainties combined and symmetrised

Signal truth: variations

- Renormalisation and factorisation scale:
  - μ_R affects α_S directly $\alpha_S(\mu_R^2) = \dfrac{\alpha_S(\mu_0^2)}{1 + \beta_0 \alpha_S(\mu_0)^2 \ln \frac{\mu_R^2}{\mu_0^2}}$
  - μ_F affects PDFs
- Evaluated as 7-point envelope

$$\{(\mu_R,\ \mu_F)\} = \{(0.5, 0.5); (0.5, 1); (1, 0.5); (1, 1); (2, 1); (1, 2); (2, 2)\}$$

- PDF and α_S:
  - Using PDF4LHC21 recommendations
    - PDF uncertainty evaluated through 100 variations
    - α_S varied between 0.118 (nominal) $\pm$ 0.001
    - Two uncertainties combined and symmetrised
- Scale uncertainty dominates

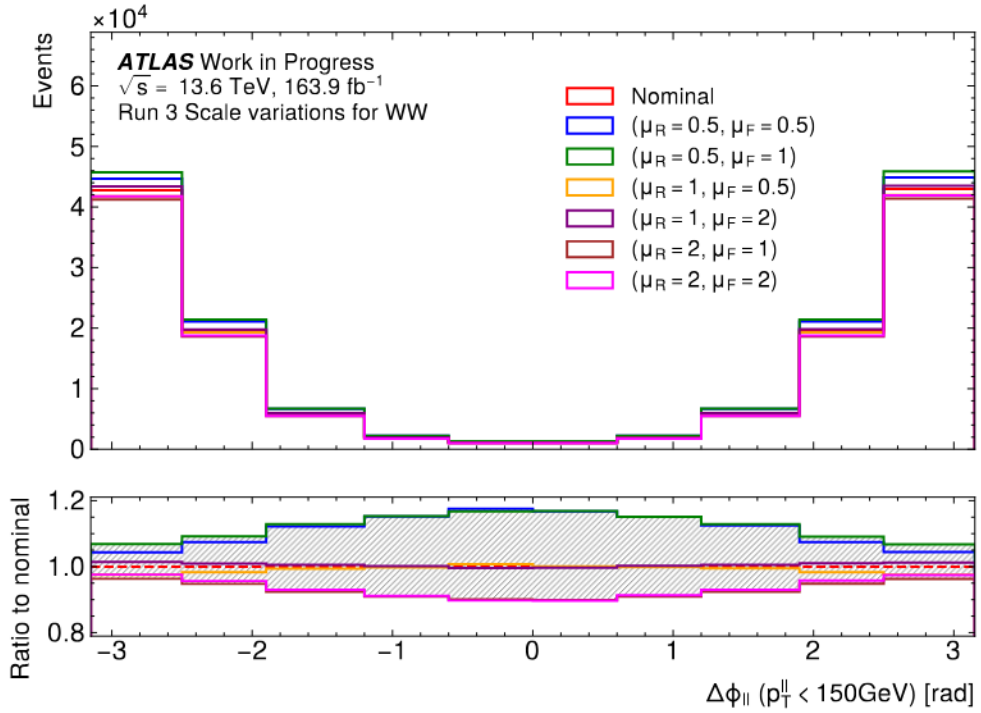

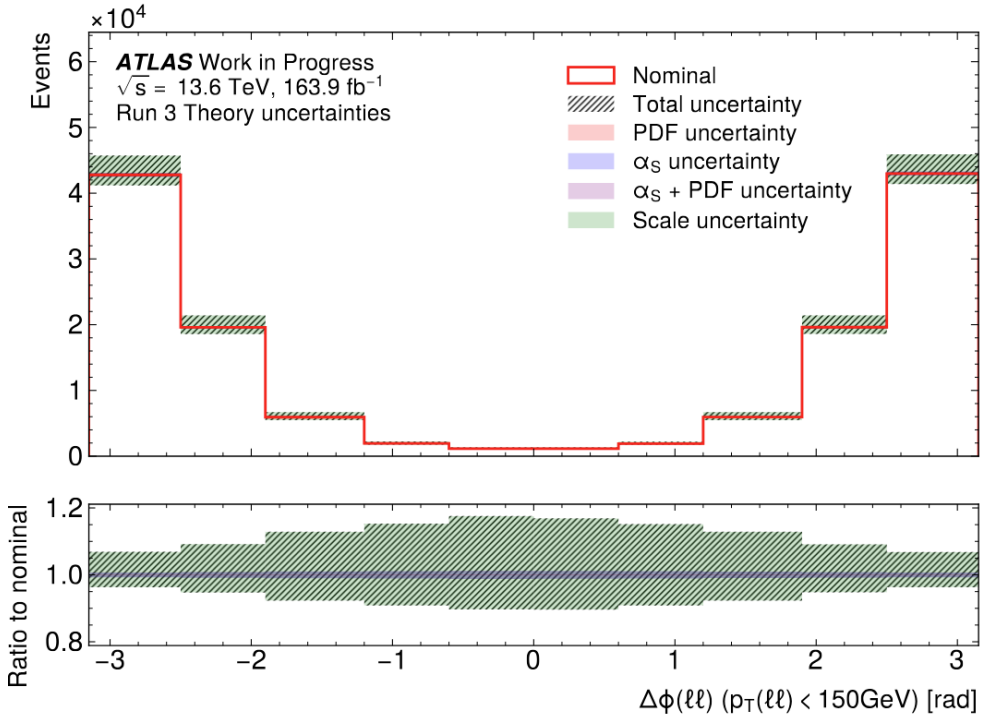

Data unfolding w/ systematics

Good agreement with Sherpa theory prediction

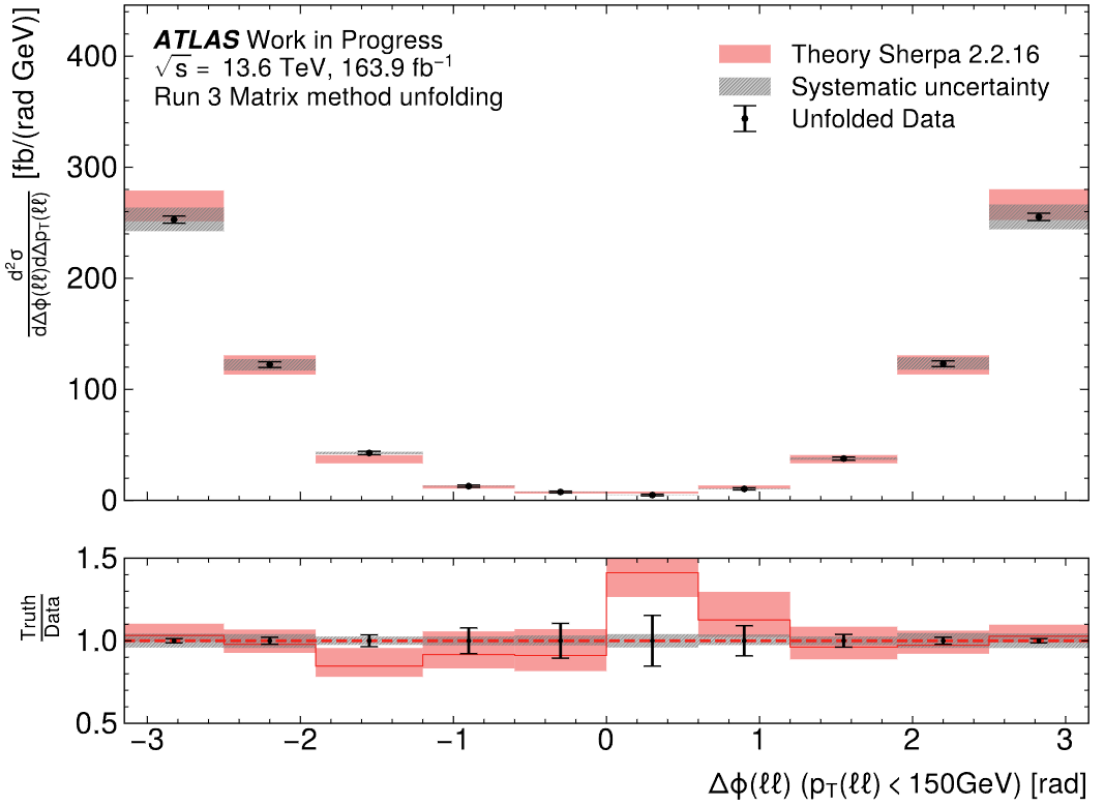

Data unfolding w/ systematics

Good agreement with Sherpa theory prediction

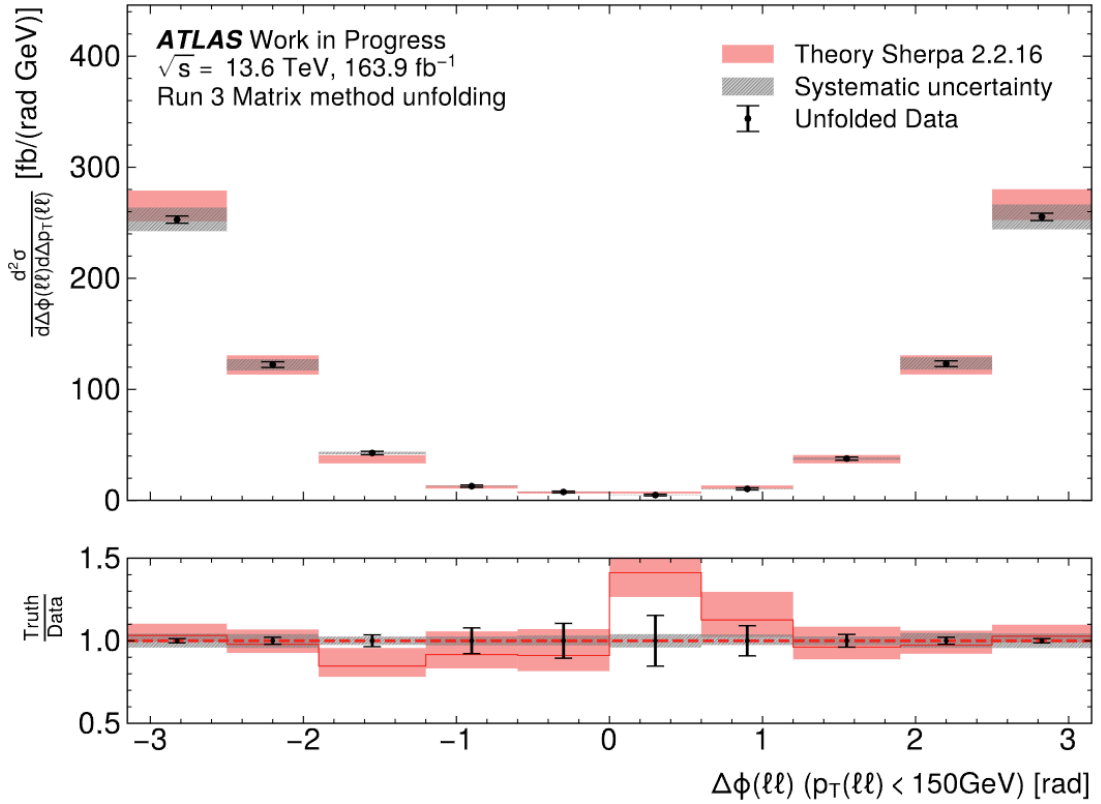

Experimental systematic uncertainty less than 5% in every bin

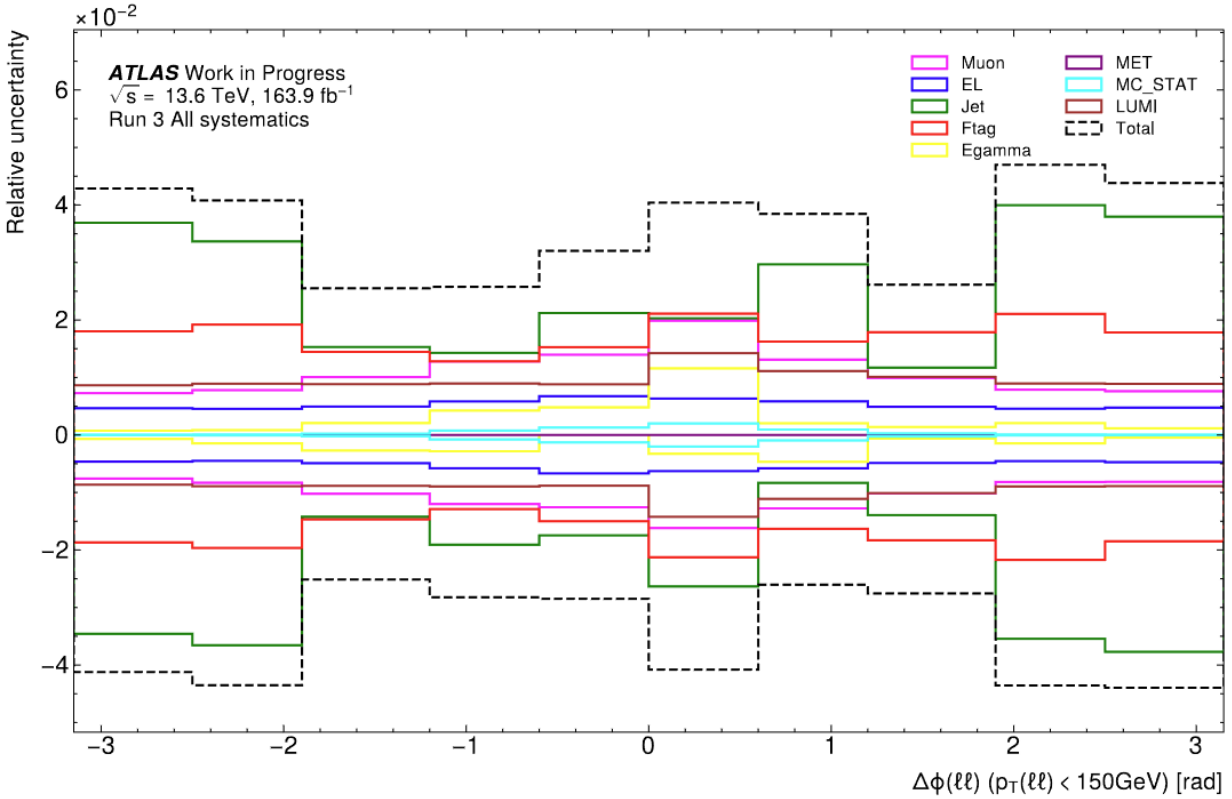

Summary and conclusions

- WW process is sensitive to potential EFT and CP-violating effects
- Presented first look into OSOF WW differential measurement with ATLAS Run3 data
  - $163\ \mathrm{fb}^{-1}$ of data -> highest recorded to date
  - Focus on enhancing sensitivity to linear EFT over previous measurements, particularly on triple gauge coupling
  - First measurement of CP-odd sensitive variables (signed $\Delta\phi(\ell\ell)$)
  - Will extend to neural network observables to probe CP-violating effects
- Good agreement between theory and prediction for CP-odd sensitive variables
- Analysis nearing ATLAS internal review, stay tuned for publication this Summer!

Thank you for your attention

Alberto Plebani

Event selection and yields

- Event selection mimics Run2 selection as close as possible, except:
  - GN2 @90% eff (before was DL1r @85%)
  - Updated isolation and identification WPs

Event selection		
Exactly 2 opposite-charged leptons ($1e$ and 1μ), $p_T > 27$GeV $\lvert\eta(e)\rvert \leq 2.47$ with crack veto $1.37 \leq \lvert\eta(e)\rvert \leq 1.52$ $\lvert\eta(\mu)\rvert \leq 2.5$		
Electrons: ID: TightLH, Isol: Tight_VarRad Muons: ID: Medium, Isol: PFlowTight_VarRad		
$\lvert d_0/\sigma_{d_0}\rvert < 5(e),\ 3(\mu),\ \lvert z_0 \cdot \sin\theta\rvert < 0.5$ mm		
No additional electron with: $p_T > 10$ GeV, $\lvert\eta\rvert \leq 2.47$, ID: LooseBLayerLH, Isol: Loose_VarRad		
No additional muon with: $p_T > 10$ GeV, $\lvert\eta\rvert \leq 2.7$, ID: Loose, Isol: NonIso		
Inclusive in jet multiplicity for $p_T(j) > 30$ GeV and $\lvert\eta(j)\rvert \leq 4.5$ JVT and fJVT applied N_{b-jets} @90% eff. (GN2 PCBT > 1) $= 0$		
$m_{e\mu} >$ 100 GeV Veto on non-prompt leptons		
Triggers:		
mc23a	mc23d	mc23e
HLT_e26_lhtight_ivarloose_L1EM22VHI HLT_e60_lhmedium_L1EM22VHI HLT_e140_lhloose_L1eEM26M HLT_mu24_ivarmedium_L1MU14FCH HLT_mu50_L1MU14FCH	HLT_e26_lhtight_ivarloose_L1eEM26M HLT_e60_lhmedium_L1eEM26M HLT_e140_lhloose_L1EM22VHI HLT_mu24_ivarmedium_L1MU14FCH HLT_mu50_L1MU14FCH	HLT_e26_lhtight_ivarloose_L1eEM26M HLT_e60_lhmedium_L1eEM26M HLT_e140_lhloose_L1EM22VHI HLT_mu24_ivarmedium_L1MU14FCH HLT_mu50_L1MU14FCH

Sample	Yields ± Stat.	Percentage (%)
WW	57 485.7 ± 77.2	34.0
$Z + jets$	3636.5 ± 324.4	2.2
WZ	2366.5 ± 9.2	1.4
VV	130.6 ± 1.1	0.1
$t\bar{t}$	77 451.1 ± 762.8	45.8
$V\gamma$	174.1 ± 25.5	0.1
$W + jets$	100.7 ± 64.6	0.1
VVV	201.1 ± 0.5	0.1
VV EWK	768.0 ± 9.0	0.5
Single-top	19 748.4 ± 28.8	11.7
Fakes	6877.6 ± 72.4	4.1
Total mc23ade	168 940.4 ± 839.2	1
Run 3 Data	170 773.0 ± 413.2	-
Data/MC	1.01	-

Fake lepton background

- Small but not insignificant contribution of fake leptons to the signal region (<10%), largely from W+jets.
- Data-driven methods were used to calculate the fake lepton background.
- The nominal fake lepton background was estimated using the asymptotic matrix method.
- Fake factor method also used to provide a systematic variation.
- Fake lepton efficiencies were calculated in a Z+jets CR
- Fake efficiencies also calculated in a ttbar CR to provide a systematic variation for fake leptons originating in heavy flavour decays.

Object	Requirment	Criteria
Lepton	p_T	> 27 GeV (Leading electron), > 10 GeV (Sub-leading electron) OR > 25 GeV (Leading muon), > 10 GeV (Sub-leading muon)
	$\|\eta\|$	< 2.47 (electron), < 2.5 (muon)
	Identification	LooseBLayerLH (electron), Loose, (muon)
	Isolation	Loose_VarRad (electron), NonIso (muon)
	Track Parameters	$\|d_0$ significance$\| < 5$ (electron), $\|z_0 \sin\theta\| < 0.5$ (electron)
	Overlap Removal	passes $e - \mu$ OR, $e - jet$ OR, passes $\mu - jet$ OR
Jet	p_T	> 35 GeV
	$\|\eta\|$	< 2.5
	b-tagging	GN2 PCBT > 1 (equivalent to 90% eff. WP), $\|\eta\| < 2.5$
	Vertex Tagging	JVT FixedEffPt WP
Event	Trigger	HLT_e26_lhtight_ivarloose_L1EM22VHI OR HLT_e60_lhmedium_L1EM22VHI OR HLT_e140_lhloose_L1EM22VHI OR HLT_e140_lhloose_L1EM22VHI OR HLT_mu24_ivarmedium_L1MU14FCH OR HLT_mu50_L1MU14FCH
	Trigger-matching	Tag-lepton required to be matched to at least one trigger decision
	Leptons	2 leptons, same flavour, opposite sign pair, no additional electrons of $p_T > 10$ GeV, LooseBLayerLH Identification and Loose_VarRad Isolation, no additional muons of $p_T > 10$ GeV, Loose Identification and NonIso Isolation
	Number of b-jets	0
	m_{ll} mass window	$\|m_Z - m_{ll}\| < 10$ GeV

Z+jets CR definition

Fake leptons VR

- Fakes VR:
  - Orthogonal to SR due to same-sign requirement on $\ell\ell$ pair
  - Good agreement in both normalisation and shape for mc23a

Sample	Yields		Percentage (%)
WW	1.6 ±		0.1
ttbar	282.2 ±		15.1
Fakes	827.6 ±		44.3
VV	596.3 ±		31.9
Single top	4.0 ±		0.2
Z+jets	57.8 ±		3.1
VVV	17.4 ±		0.9
VV+jets	83.3 ±		4.5
Vgamma	0.1 ±		0.0
Total	1870.2 ±	nan	1
Data	1870.0 ±	43.2	-
Data/MC	1.00		-

Object	Requirment	Criteria
Lepton	p_T	> 27 GeV (electron), > 27 GeV (muon)
	$\|\eta\|$	< 2.47 (electron), < 2.5 (muon)
	Identification	TightLH (electron), Medium, (muon)
	Isolation	Tight_VarRad (electron), PflowTight_VarRad (muon)
	Track Parameters	$\|d_0$ significance$\| < 5$ (electron), $\|d_0$ significance$\| < 3$ (muon), $\|z_0 \sin\theta\| < 0.5$
	Overlap Removal	passes $e-\mu$ OR, $e-jet$ OR, passes $\mu-jet$ OR
Jet	p_T	> 30 GeV
	$\|\eta\|$	< 4.5
	b-tagging	GN2 PCBT > 1 (equivalent to 90% eff. WP), $\|\eta\| < 2.5$
	Vertex Tagging	JVT FixedEffPt WP
Event	Trigger	HLT_e26_lhtight_ivarloose_L1EM22VHI OR HLT_e60_lhmedium_L1EM22VHI OR HLT_e140_lhloose_L1EM22VHI OR HLT_e140_lhloose_L1EM22VHI OR HLT_mu24_ivarmedium_L1MU14FCH OR HLT_mu50_L1MU14FCH
	Leptons	1 electron and 1 muon of same sign, no additional electrons of $p_T > 10$ GeV, LooseBLayerLH Identification and Loose_VarRad Isolation, no additional muons of $p_T > 10$ GeV, Loose Identification and NonIso Isolation
	Number of b-jets	0
	$m_{e\mu}$	> 85 GeV

ttbar background

- Ttbar constitutes the largest background in the signal region
- A data-driven approach known as b-tag counting was used to estimate it.
- This approach was adopted in the Run 2 WW analysis.
- Ttbar yields are derived from data in 2b-jet and 1b-jet CRs
- The yield in the 0b-jet signal region is estimated by exploiting correlation effects between the 1b and 2b CR yields

$$N_{1b}^{t\bar{t}} = N_{1b} - N_{1b}^{\text{others}} = N_{\geq 0b}^{t\bar{t}} \cdot 2\varepsilon_b \left(1 - C_b \varepsilon_b\right) ,$$
$$N_{2b}^{t\bar{t}} = N_{2b} - N_{2b}^{\text{others}} = N_{\geq 0b}^{t\bar{t}} \cdot C_b \varepsilon_b^2 ,$$
$$N_{0b}^{t\bar{t}} = N_{\geq 0b}^{t\bar{t}} \cdot \left(1 - 2\varepsilon_b + C_b \varepsilon_b^2\right) ,$$

$$N_{0b}^{t\bar{t}} = \frac{C_b}{4} \frac{\left(N_{1b}^{t\bar{t}} + 2N_{2b}^{t\bar{t}}\right)^2}{N_{2b}^{t\bar{t}}} - N_{1b}^{t\bar{t}} - N_{2b}^{t\bar{t}} ,$$

$$C_b = 4 \cdot N_{\text{MC}}^{t\bar{t}} N_{2b,\text{MC}}^{t\bar{t}} / \left(N_{1b,\text{MC}}^{t\bar{t}} + 2 \cdot N_{2b,\text{MC}}^{t\bar{t}}\right)^2 ,$$

ttbar VR

- ttbar VR:
  - Extra cuts at $m_{lj} < 140\ GeV$ and $\Delta\phi(e\mu) < \pi/2$
- Good agreement in shape and normalisation

Sample	Yields		Percentage (%)
WW	223.1 ±		17.6
ttbar	810.0 ±		64.0
Fakes	51.8 ±		4.1
VV	25.5 ±		2.0
Single top	146.1 ±		11.5
Z+jets	5.5 ±		0.4
VVV	1.2 ±		0.1
VV+jets	2.9 ±		0.2
Vgamma	0.1 ±		0.0
Total	1266.3 ±	95.2	1
Data	1357.0 ±	36.8	-
Data/MC	1.07		-

Object	Requirment	Criteria
Lepton	p_T	> 27 GeV (electron), > 27 GeV (muon)
	$\|\eta\|$	< 2.47 (electron), < 2.5 (muon)
	Identification	TightLH (electron), Medium, (muon)
	Isolation	Tight_VarRad (electron), PflowTight_VarRad (muon)
	Track Parameters	$\|d_0$ significance$\| < 5$ (electron), $\|d_0$ significance$\| < 3$ (muon), $\|z_0 \sin\theta\| < 0.5$
	Overlap Removal	passes $e-\mu$ OR, $e-jet$ OR, passes $\mu-jet$ OR
Jet	p_T	> 30 GeV
	$\|\eta\|$	< 4.5
	b-tagging	GN2 PCBT > 1 (equivalent to 90% eff. WP), $\|\eta\| < 2.5$
	Vertex Tagging	JVT FixedEffPt WP
Event	Trigger	HLT_e26_lhtight_ivarloose_L1EM22VHI OR HLT_e60_lhmedium_L1EM22VHI OR HLT_e140_lhloose_L1EM22VHI OR HLT_e140_lhloose_L1EM22VHI OR HLT_mu24_ivarmedium_L1MU14FCH OR HLT_mu50_L1MU14FCH
	Leptons	1 electron and 1 muon of opposite charge, no additional electrons of $p_T > 10$ GeV, TightLH Identification and Tight_VarRad Isolation, no additional muons of $p_T > 10$ GeV, Medium Identification and PflowTight_VarRad Isolation
	Number of b-jets	0
	$m_{e\mu}$	> 85 GeV
	$m_{\ell j}$	< 140 GeV
	$\Delta\phi_{e\mu}$	$< \pi/2$

Unfolding: bias uncertainty and closure

- Data-driven bias uncertainty
  - Obtained by reweighting MC to reflect data
- Closure test:
  - Unfold MC-to-MC
  - Perfect closure observed

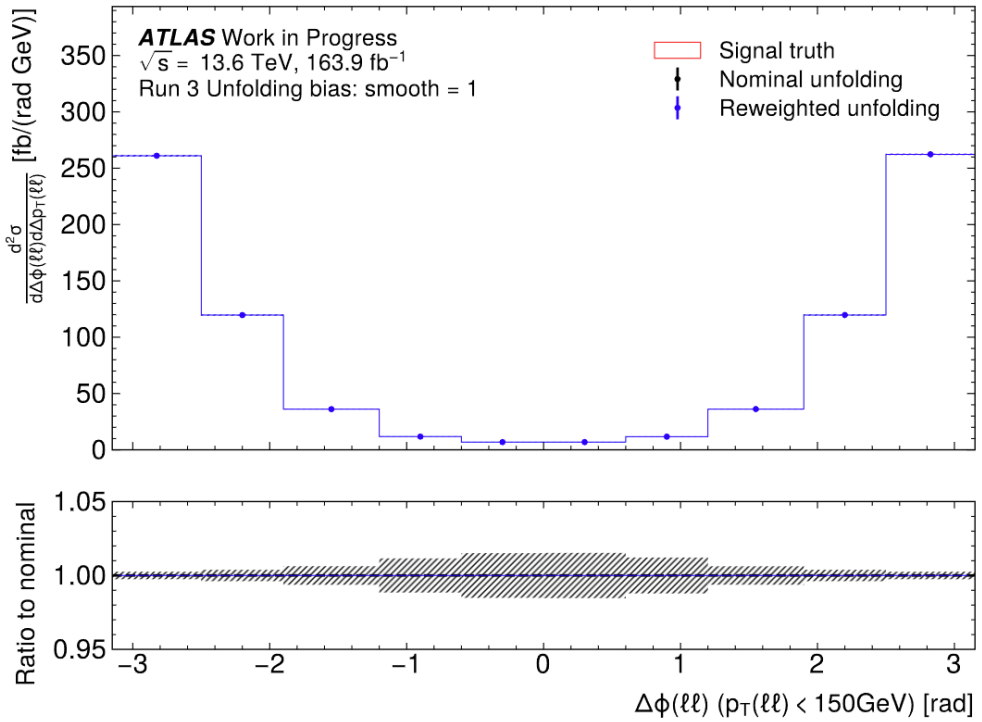

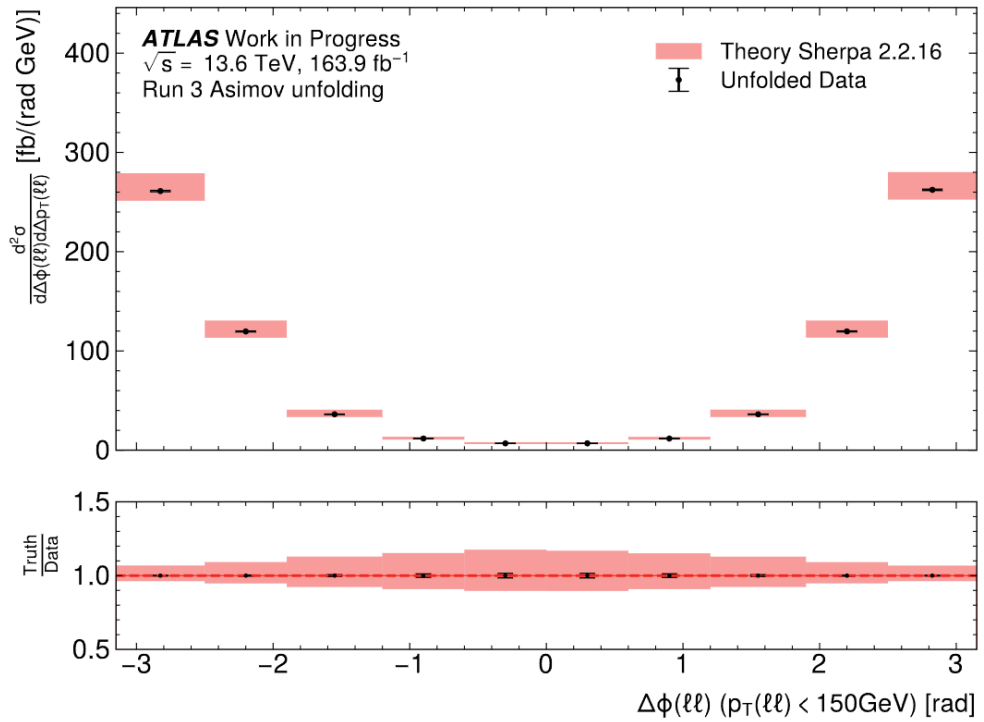

Unfolding setup

- Unfolding performed using custom-made IBU script with RooUnfold
- Bin optimised so that each bin has at least 500 entries **and** at least 70% in diagonal of the migration matrix (details in backup)
- Performed unfolding both MC-to-MC (closure test) and using real Data
  - For fakes, using both MC and data-driven fakes estimation
  - Plan to include data-driven estimation also for ttbar
- Uncertainties:
  - All instrumental systematics added
  - Currently working on theoretical (PDF and scale)
- Added theoretical uncertainties on the truth distribution

Theory: scale uncertainties calculation

- Scale variations:
  - 7-point envelope:
    - $\{(\mu_R,\ \mu_F)\} = \{(0.5, 0.5); (0.5, 1); (1, 0.5); (1, 1); (2, 1); (1, 2); (2, 2)\}$

Nominal

- Ex. for signal $W^+W^- \to e^{\pm}\nu\mu^{\mp}\nu$ (701050, *Sh_llvv_os*):
  - Take syst-variated reco and truth for each pair of μ_R and μ_F and calculate MM, efficiency, and acceptance
  - Take NOSYS for backgrounds to subtract from data
  - Unfold the syst-variated truth
  - Get the uncertainty
- Repeat for all processes (WZ, ttbar, Zee, and so on) independently
  - Still not fully implemented

Theory: PDF uncertainties calculation

- Working with the 100 NNPDF variations, combining them according to PDF4LHC21 recs:
  - (N_eig = 100)

$$\delta^{\mathrm{pdf}}\mathcal{F} = \sqrt{\sum_{k=1}^{N_{\mathrm{eig}}} \left(\mathcal{F}^{(k)} - \mathcal{F}^{(0)}\right)^2}$$

  - Two extra variations for $\alpha_S = 0.117$ and $\alpha_S = 0.119$ (nominal is $\alpha_S = 0.118$)

$$\delta^{\alpha_s}\sigma = \frac{\sigma(\alpha_s = 0.119) - \sigma(\alpha_s = 0.117)}{2},$$

  - Combining the two:
    - $$\delta^{\mathrm{PDF}+\alpha_s}\sigma = \sqrt{(\delta^{\mathrm{pdf}}\sigma)^2 + (\delta^{\alpha_s}\sigma)^2}\,.$$

- Consider together all processes with the same PDF set
  - Ex. take all Sherpa processes which use NNPDF3.0 NNLO Hessian PDF set, change reco and truth (only if signal) and calculate MM, efficiency, and acceptance. Use the syst-variated estimation of the backgrounds (if affected, if not consider NOSYS) and unfold
    - Obtain one uncertainty for every group of PDF (NNPDF3.0 NLO Hessian, NNPDF3.0 NLO 4FS, NNPDF3.0 NLO, NNPDF3.0 NNLO Hessian, NNPDF3.0 NNLO 4FS)
  - Currently implemented only for signal, working on adding others

Theory uncertainties

DSID	Process	Generator	Nominal Hessian PDF	PDF set	PDF for scale	PDF set for scale	Scale variations names
522024	$t\bar{t}Z(\to e\bar{e})$	MadGraph	93300 (40 + 2 for α_S)	PDF4LHC21_40	303000	NNPDF NLO Hessian	MUR10_MUF20
522028	$t\bar{t}Z(\to \mu\bar{\mu})$	MadGraph	93300 (40 + 2 for α_S)	PDF4LHC21_40	303000	NNPDF NLO Hessian	MUR10_MUF20
522032	$t\bar{t}Z(\to \tau\bar{\tau})$	MadGraph	93300 (40 + 2 for α_S)	PDF4LHC21_40	303000	NNPDF NLO Hessian	MUR10_MUF20
525955	tWZ	MadGraph	93300 (40 + 2 for α_S)	PDF4LHC21_40	303000	NNPDF NLO Hessian	MUR10_MUF20
545027	tZq	MadGraph	93700 (40 + 2 for α_S)	PDF4LHC21_40_4FS	260400	NNPDF NLO 4FS	MUR10_MUF20
545028	$\bar{t}Zq$	MadGraph	93700 (40 + 2 for α_S)	PDF4LHC21_40_4FS	260400	NNPDF NLO 4FS	MUR10_MUF20
601230	$t\bar{t}$	PowhegPythia	93300 (40 + 2 for α_S)	PDF4LHC21_40	260000	NNPDF NLO	MUR1_MUF2
601354	tW	PowhegPythia	93300 (40 + 2 for α_S)	PDF4LHC21_40	260000	NNPDF NLO	MUR1_MUF2
700772	$\tau\tau\gamma$	Sherpa	93300 (40 + 2 for α_S)	PDF4LHC21_40	303200	NNPDF NNLO Hessian	MUR1_MUF2_PDF303200_PSMUR1_PSMUF2
700792	$Z \to \tau\bar{\tau}$ (+B)	Sherpa	93300 (40 + 2 for α_S)	PDF4LHC21_40	303200	NNPDF NNLO Hessian	MUR1_MUF2_PDF303200_PSMUR1_PSMUF2
700793	$Z \to \tau\bar{\tau}$ (+C)	Sherpa	93300 (40 + 2 for α_S)	PDF4LHC21_40	303200	NNPDF NNLO Hessian	MUR1_MUF2_PDF303200_PSMUR1_PSMUF2
700794	$Z \to \tau\bar{\tau}$ (+ LF)	Sherpa	93300 (40 + 2 for α_S)	PDF4LHC21_40	303200	NNPDF NNLO Hessian	MUR1_MUF2_PDF303200_PSMUR1_PSMUF2
700901	$Z \to \tau\bar{\tau}$ low_Mll (+B)	Sherpa	93300 (40 + 2 for α_S)	PDF4LHC21_40	303200	NNPDF NNLO Hessian	MUR1_MUF2_PDF303200_PSMUR1_PSMUF2
700902	$Z \to \tau\bar{\tau}$ low_Mll (+C)	Sherpa	93300 (40 + 2 for α_S)	PDF4LHC21_40	303200	NNPDF NNLO Hessian	MUR1_MUF2_PDF303200_PSMUR1_PSMUF2
700903	$Z \to \tau\bar{\tau}$ low_Mll (+LF)	Sherpa	93300 (40 + 2 for α_S)	PDF4LHC21_40	303200	NNPDF NNLO Hessian	MUR1_MUF2_PDF303200_PSMUR1_PSMUF2
700997	$t\bar{t}W$	Sherpa	93300 (40 + 2 for α_S)	PDF4LHC21_40	303200	NNPDF NNLO Hessian	MUR1_MUF2_PDF303200_PSMUR1_PSMUF2
701000	$\ell\ell\ell\ell jj$ (EW)	Sherpa	93300 (40 + 2 for α_S)	PDF4LHC21_40	303200	NNPDF NNLO Hessian	MUR1_MUF2_PDF303200_PSMUR1_PSMUF2
701005	$\ell\ell\ell\nu jj$ (EW)	Sherpa	93300 (40 + 2 for α_S)	PDF4LHC21_40	303200	NNPDF NNLO Hessian	MUR1_MUF2_PDF303200_PSMUR1_PSMUF2
701010	$\ell\ell\nu\nu jj$ (OS) (EW)	Sherpa	93300 (40 + 2 for α_S)	PDF4LHC21_40	303200	NNPDF NNLO Hessian	MUR1_MUF2_PDF303200_PSMUR1_PSMUF2
701020	$\ell\ell\ell\ell jj$ (Int. EW)	Sherpa	93300 (40 + 2 for α_S)	PDF4LHC21_40	303200	NNPDF NNLO Hessian	MUR1_MUF2_PDF303200_PSMUR1_PSMUF2
701025	$\ell\ell\ell\nu jj$ (Int. EW)	Sherpa	93300 (40 + 2 for α_S)	PDF4LHC21_40	303200	NNPDF NNLO Hessian	MUR1_MUF2_PDF303200_PSMUR1_PSMUF2
701030	$\ell\ell\nu\nu jj$ (OS) (Int. EW)	Sherpa	93300 (40 + 2 for α_S)	PDF4LHC21_40	303200	NNPDF NNLO Hessian	MUR1_MUF2_PDF303200_PSMUR1_PSMUF2
701040	$\ell\ell\ell\ell$	Sherpa	93300 (40 + 2 for α_S)	PDF4LHC21_40	303200	NNPDF NNLO Hessian	MUR1_MUF2_PDF303200_PSMUR1_PSMUF2
701045	$\ell\ell\ell\nu$	Sherpa	93300 (40 + 2 for α_S)	PDF4LHC21_40	303200	NNPDF NNLO Hessian	MUR1_MUF2_PDF303200_PSMUR1_PSMUF2
701050	$\ell\nu\ell\nu$ (OS)	Sherpa	93300 (40 + 2 for α_S)	PDF4LHC21_40	303200	NNPDF NNLO Hessian	MUR1_MUF2_PDF303200_PSMUR1_PSMUF2
701085	$Z(\to qq)Z(\to \ell\ell)$	Sherpa	93300 (40 + 2 for α_S)	PDF4LHC21_40	303200	NNPDF NNLO Hessian	MUR1_MUF2_PDF303200_PSMUR1_PSMUF2
701090	$Z(\to bb)Z(\to \ell\ell)$	Sherpa	93300 (40 + 2 for α_S)	PDF4LHC21_40	303200	NNPDF NNLO Hessian	MUR1_MUF2_PDF303200_PSMUR1_PSMUF2
701105	$W(\to qq)Z(\to \ell\ell)$	Sherpa	93300 (40 + 2 for α_S)	PDF4LHC21_40	303200	NNPDF NNLO Hessian	MUR1_MUF2_PDF303200_PSMUR1_PSMUF2
701165	$\ell\ell\gamma jj$	Sherpa	93300 (40 + 2 for α_S)	PDF4LHC21_40	303200	NNPDF NNLO Hessian	MUR1_MUF2_PDF303200_PSMUR1_PSMUF2
700866	$WWW \to \ell\ell\ell\nu\nu\nu$	Sherpa	93700 (40 + 2 for α_S)	PDF4LHC21_40_4FS	261400	NNPDF NNLO 4FS	MUR1_MUF2_PDF303200_PSMUR1_PSMUF2
700867	$WZZ \to \ell\ell\ell\nu\nu\nu$	Sherpa	93700 (40 + 2 for α_S)	PDF4LHC21_40_4FS	261400	NNPDF NNLO 4FS	MUR1_MUF2_PDF303200_PSMUR1_PSMUF2

Iterative Bayesian Unfolding

- Assume an initial hypothesis for the probability density of the truth distribution f(t)
  - $f(t) = \int dr\ g(r)\ P(t|r)$, with $g(r)$ taken from data and $P(t|r)$ taken from MC simulations
  - $P(t|r)$ is then updated iteratively as
  - The n^{th} step is obtained as

$$P(t|r) = \frac{P(r|t)f(t)}{\int f(t)P(r|t)dt} = \frac{P(r|t)f(t)}{g(r)}$$

$$f^{n+1}(t) = \int f^{r}(t)\frac{g(r)_{\text{data}}}{g^{n}(r)}P(r|t)dt$$

  - Procedure repeated until difference between $f^{n+1}(t)$ and $f(t)$ is less than a certain threshold

Bootstrap

- Implemented bootstrap technique in unfolding calculation to estimate statistical uncertainty
- Error comparison:
  - Stat_uncertainty is the error coming from the “nominal” unfolding
  - Bootstrap_error is the one coming from the bootstrap
  - Comparable, with bootstrap being usually smaller

```
(Pdb) print(np.array(stat_uncertainty))
[39.66092158 35.32825551 46.28077764 59.5925267  71.00373422 80.09907369
 86.42675813 84.24197714 88.01504912 89.05609265 87.59173586 83.66074768
 81.72525735 77.31381775 77.15241043 73.69661204 65.25220743 60.70280759
 54.10084857 48.68811855 46.06392141 40.08269998 36.10017056 28.05210092
 27.99039308 25.7299486  30.99368253]
(Pdb) print(np.array(bootstrap_error))
[38.44243091 35.37961289 45.79619605 59.46766351 72.612459   78.36038555
 87.00428931 82.43005963 85.84026613 87.6244471  85.96676988 84.16738236
 82.73307236 76.96109972 73.74238683 76.0298312  65.82961615 61.14980692
 55.00073527 47.50449302 47.10482908 39.70725019 35.10139281 28.12479942
 27.75629444 26.1913554  32.08084817]
(Pdb) difference_error = bootstrap_error - stat_uncertainty
(Pdb) print(np.array(difference_error / stat_uncertainty))
[-0.0307227   0.00145372 -0.01047047 -0.00209528  0.0226569  -0.02170672
  0.00668232 -0.02150849 -0.02470922 -0.01607577 -0.01855159  0.00605582
  0.01233174 -0.00456216 -0.04419854  0.03165979  0.00884888  0.00736373
  0.0166335  -0.02431036  0.02259703 -0.00936688 -0.02766684  0.00259155
 -0.00836354  0.01793267  0.03507701]
```

7.1.3 Bootstrap techniques for statistical uncertainty

The statistical uncertainty on the unfolded distribution is estimated using the bootstrap method. For this, the `BootstrapGenerator` package [22] was used. This method consists of generating a set of replicas of the measured spectrum, all derived by fluctuating each event in the data distribution by a Poisson distribution centred around the value of the measured data. In practice, this is obtained by performing the following steps:

- Generate a response by using the background-subtracted-data as per Eq. (7.15)
- For every bin in the data distribution, get the total number of expected events N_{meas} as the number of measured data events
- Sample N_{meas} times a weight $\omega_i \sim \text{Poisson}(1)$ from a Poisson distribution with mean 1, and fill the new histogram with these weights
- Repeat this procesure 1000 times. Now every bin will have entries distributed according to a Poisson distribution centred around the measured number of events.
- For every replica ($i = 1, \ldots, 1000$), do:
- 1. Get the reweighted data distribution
  2. Build a reweighted background-subtracted data using Eq. (7.15)
  3. Unfold the reweighted background-subtracted data to the truth with the nominal response
  4. Store the entries of the new unfolded distribution
- Once the loop is completed, the uncertainty in each bin j from the 1000 variations is cpmputed as the RMS of all the variations, as per Eq. (7.16), where $N = 1000$, x_i^j are the entries from the i-th variation in the j-th bin, and $\bar{x}^j$ refers to the entries in the j-th bin of the nominal unfolded distribution.

$$\sigma_U^j = \sqrt{\frac{1}{N-1}\sum_{i=1}^{N}(x_i^j - \bar{x}^j)^2} \tag{7.16}$$

Dim-6 SMEFT interpretation

- Plan to do EFT interpretation on **CP-even/odd dim-6 operators**
  - Set limits on 4 Wilson coefficients: **cW, cHWB, cWtil, CHWBtil**
  - mc23a/d/e samples requested for **linear, quadratic and cross terms**
  - MC request in EW subgroup and the production JIRAticket
    - mc23a/d are done, waiting for some tails in mc23e to finish

- The cross-section prediction in each bin:

$$f^b_{\text{pred}}(\boldsymbol{c},\boldsymbol{\theta}) = f^b_{\text{pred, SM}}\left(1 + \sum_i A_{bi}\frac{c_i}{\Lambda^2} + \sum_i B_{bi}\frac{c_i^2}{\Lambda^4} + \sum_{i<j} C_{bij}\frac{c_i c_j}{\Lambda^4}\right)\prod_n^{n_{\text{theory,syst}}}(1+u_n\theta_n)$$

linear quadratic Cross

- The Likelihood function for EFT fit

$$L(\mathbf{x}\mid\mathbf{c},\boldsymbol{\theta}) = \frac{1}{\sqrt{(2\pi)^{n_{\text{bins}}}\det(V)}}\exp\left(-\frac{1}{2}\Delta\mathbf{x}^{\top}(\mathbf{c},\boldsymbol{\theta})\,V^{-1}\,\Delta\mathbf{x}(\mathbf{c},\boldsymbol{\theta})\right)\times\prod_{i=1}^{n_{\text{theo syst}}} f_i(\theta_{\text{theo syst},i})\times\prod_{i=1}^{n_{\text{exp syst}}} f_i(\theta_{\text{exp syst},i})$$

EFT interpretation: plan

- Fitting tool: EFT-fun Fit setup:
  - Unfolded distributions of **mll** (only mc23a used for this preliminary study)
    - Not particularly sensitive to EFT effects, used mainly to validate the framework and because we expect low sensitivity
  - EFT formulation only linear effect
  - Stat uncertainty on unfolded data - embedded in covariance matrix *V*
  - Experimental uncertainties on unfolded data - treated as NPs
  - Theoretical uncertainties on prediction - treated as NPs
- Will perform EFT study on $\Delta\phi(\ell\ell)$ which gives us sensitivity to CP-even and CP-odd operators
  - Will also add ONN which is expected to improve this even further

CPV in EFT

- EFT extensions to SM add CP-violating operators to the SM lagrangian
- The leading order BSM term in the matrix element is the interference between SM and EFT

$$\mathcal{L} = \mathcal{L}_{\mathrm{SM}} + \sum_i \frac{c_i}{\Lambda^2}\tilde{\mathcal{O}}_i \longrightarrow |\mathcal{M}_{\mathrm{BSM}}|^2 = |\mathcal{M}_{\mathrm{SM}}|^2 + 2\mathrm{Re}\{\mathcal{M}_{\mathrm{SM}}\mathcal{M}^{\star}_{\mathrm{d6}}\} + |\mathcal{M}_{\mathrm{d6}}|^2$$

- CP-odd EFT operators => interference is also CP-odd
- Interference can be constructive or destructive
- Kinematic similarities between constructive and destructive interference events means that if the variable is insensitive to CP-odd nature (ex. pT), the interference effects cancel out
- Sensitivity can be “resurrected” by studing CP-odd sensitive observables [arxiv.708.07823]

Neural Network variable

- arxiv.2112.05052 and arxiv.2209.05143: ML models can be used to construct complex observables that are sensitive to CP-odd asymmetries
- By training a multi-class NN to classify constructive, destructive and SM events, a CP-sensitive observable can be defines as:
  - $O_{NN} = P_{+} - P_{-}$